Characterisation of synergistic and antagonistic petrol component chemical class effects on octane blending behaviour

by

David Ken Leigh

Thesis presented in partial fulfilment of the requirements for the degree of Master of Engineering (Mechanical) in the Faculty of Engineering at Stellenbosch University

Supervisor: Mr. R. Haines
Co-supervisor: Dr. G. Floweday

March 2020

Declaration

By submitting this thesis electronically, I declare that the entirety of the work contained therein is my own, original work, that I am the sole author thereof (save to the extent explicitly otherwise stated), that reproduction and publication thereof by Stellenbosch University will not infringe any third party rights and that I have not previously in its entirety or in part submitted it for obtaining any qualification.

Date: March 2020

Abstract

Characterisation of synergistic and antagonistic petrol component chemical class effects on octane blending behaviour

D.K. Leigh

Department of Mechanical and Mechatronic Engineering,
University of Stellenbosch,
Private Bag X1, Matieland 7602, South Africa.

Thesis: MEng (Mech)

March 2020

Knock free operation has influenced the development of internal combustion (IC) engine technology and spark ignition (SI) fuels. Knock is the noise associated with the harmful and abnormal combustion phenomenon known as autoignition. For a given engine configuration, the propensity of knock in IC engines depends primarily on the anti-knock quality of the fuel. Research octane number (RON) and motor octane number (MON) are measured fuel properties indicating a fuel's resistance to autoignition. Fuel producers ultimately seek to produce fuels with RON and MON values suitable for modern IC engines, however, the highly complex non-linear blending interactions between the constituents of the fuel recipe make this challenging.

The present research was undertaken to characterise the non-linear synergistic and antagonistic octane blending behaviours between important common chemical class components, carefully selected to represent the SI fuel recipe on a fundamental level. The RON and MON values for all binary combinations of these components at various blend ratios were measured using Stellenbosch University's uniquely modified Cooperative Fuels Research engine. All oc-

tane experiments were performed in accordance with the American Society for Testing and Materials D2699 and D2700 standards.

The measured RON and MON data showed results consistent with the literature and highlighted a shortage of research data for some binary blends. The project hypothesis was supported, showing that non-linearities do exist in octane blending between binary combinations and that more than one non-linearity can exist in a binary blend. Using this and the measured data, conclusions were drawn on the links between the various chemical classes, blending ratios and the non-linearities in octane number. It was demonstrated that octane sensitivity is a function of blend ratio and provides insight into improving fuel recipes for modern SI engines.

The octane boosting capabilities of a non-metallic octane booster, was shown to significantly boost the octane of some of the selected components and had no significant effect on others. It was found to influence the RON value more than the MON value of a blend.

The suitability of two well established empirical octane prediction models were investigated for use in predicting octane. The predicted data was compared to the measured data and deficiency in the better performing model was identified and then optimised to improve the octane predictions for the binary blends.

Uittreksel

Karakterisering van saamwerkende en teenstrydige petrol komponent chemiese klas effekte op oktaan vermengingsgedrag

D.K. Leigh

Departement Meganiese en Megatroniese Ingenieurswese,
Universiteit van Stellenbosch,
Privaatsak X1, Matieland 7602, Suid Afrika.

Tesis: MIng (Meg)

Maart 2020

Die ontwikkeling van binnebrand motor-tegnologie en vonkontsteking (VO) brandstowwe word beïnvloed deur die vereiste vir klopvrye werking van die enjin. Klop is die geraas verwant aan die skadelike en abnormale verbrandingsverskynsel wat bekend staan as 'outo-ontsteking'. Die neiging tot klop vir 'n gegewe binnebrand motor konfigurasie, is hoofsaaklik afhanklik van die anti-klop kwaliteit van die brandstof. Die navorsingsoktaansyfer (NOS) en motoroktaansyfer (MOS) is meetbare brandstof eienskappe wat 'n aanduiding gee van die brandstof se weerstand teen outo-ontsteking. Brandstof vervaardigers poog om brandstowwe, met gepaste NOS en MOS waardes, vir moderne binnebrand motors te vervaardig, hoewel die hoogs gekompliseerde meng interaksies tussen die samestellende komponente van die brandstofresep 'n uitdaging is.

Die huidige navorsing is onderneem om die nie-lineêre saamwerkende en teenstrydige oktaan meng gedragte tussen belangrike alledaagse chemise-klas komponente te karakteriseer. Die voorafgaande is sorgvuldig gekies om die VO brandstofresep op 'n fundamentele vlak te verteenwoordig. Die NOS en MOS waardes vir alle binêre kombinasies van hierdie komponente is gemeet by verskeie mengselverhoudings met behulp van die Universiteit van Stellen-

bosch se uniek gewysigde Samewerkende Brandstof Navorsings (SBN) motor. Alle oktaan eksperimente is uitgevoer in ooreenstemming met die Amerikaanse Vereniging vir Toetsing en Materiale se D2699 en D2700 standaarde.

Die afgemete NOS en MOS data het resultate gelewer wat konsekwent is met die literatuur en het die tekort aan navorsingsdata vir binêre mengsels beklemtoon. Die projek se hipotese is ondersteun deur te toon dat nie-lineêre gedrag wel bestaan in oktaan menging tussen binêre kombinasies van die komponente en dat meer as een nie-lineêre verwantskap (saamwerkend en teenstrydig) kan bestaan in so 'n mengsel kombinasie. Deur gebruik te maak van hierdie resultaat en die afgemete data, is daar gevolgtrekkings gemaak met betrekking tot die verwantskap tussen verskeie chemiese klasse, mengsel verhoudings en die nie-lineêriteite in die oktaan syfer. Daar is gedemonstreer dat oktaan sensitiwiteit 'n funksie van meng-verhoudings is wat bydra tot die verbetering van brandstofresepte vir moderne VO motors.

Die oktaan aanjagingsvermoë van 'n nie-metaal oktaan aanjaer (NMOA) het 'n beduidende verhewing in die oktaan van sekere van die geselekteerde komponente gehad, terwyl dit geen beduidende effek op ander gehad het nie. Daar is gevind dat dit 'n groter invloed op die NOS waarde van 'n mengsel het as wat dit op die MOS waarde van 'n mengsel het.

Die gepastheid van twee goed gevestigde empiriese oktaan-voorspellingsmodelle is ondersoek. Die voorspelde data is vergelyk met die afgemete data en tekortkominge in die model wat die beste gepresteer het, is geïdentifiseer en is vervolgens geoptimeer om by te dra tot die verbetering van oktaan voorspellings vir binêre mengsels.

Dedication

To you dad.

Acknowledgements

Mr. Richard Haines and Dr. Gareth Floweday
Thank you for your supervision, patience and continued encouragement throughout this project.

Sasol Fuels Application Center
I would like to thank the SFAC for the opportunity of a lifetime and for providing adequate financial support.

Mr. Reynaldo Rodriquez
Your input into this project is greatly appreciated.

Department of Mechanical and Mechatronic Engineering
Thank you to all of the staff who made valuable contributions to this project.

Contents

List of Figures

List of Tables

Nomenclature

Abbreviations

AFR	Air-fuel ratio
API	American Petroleum Institute
ASTM	American Society for Testing and Materials
BON	Blended octane number
CAS	Chemical Abstract Service
CC	Characteristic curve
C-C	Carbon-carbon
CF2	Clean Fuels II
CFR	Cooperative Fuels Research
C-H	Carbon-hydrogen
CR	Compression ratio
DIN	German Institute for Standardisation
ECU	Engine control unit
EIS	Electronic ignition system
ETBE	Ethyl tert-butyl ether

FBR	Full boiling range
GC-MS	Gas chromatography-mass spectrometry
IAT	Intake air temperature
IC	Internal combustion
KI	Knock intensity
LBV	Linear-by-volume
MIXT	Mixture temperature
MON	Motor octane number
MTBE	Methyl tert-butyl ether
NMOB	Non-metallic octane booster
NTC	Negative temperature coefficient
OI	Octane index
ON	Octane number
OS	Octane sensitivity
PPE	Personal protection equipment
PRF	Primary reference fuel
RCM	Rapid compression machine
RON	Research octane number
SE	Standard error
SFA	Sasol fuel alcohol
SFAC	Sasol Fuels Application Center

SI	Spark ignition
TAME	Tertiary amyl methyl ether
TEL	Tetra-ethyl lead
TRF	Toluene reference fuel
TSF	Toluene standardised fuel
ULP	Unleaded petrol

Chapter 1

Introduction

1.1 Background

There is little doubt that the internal combustion (IC) engine has changed the face of the earth. The scarcity of oil and gas reserves has forced the automotive industry to focus its efforts on minimizing fuel consumption and emission gasses to sustainably meet consumer demands (Gheorghiu, 2012). The transport sector accounted for one-fourth of the total emissions in 2016 (71 % larger than in 1990) and 25 % of the total worldwide carbon dioxide (CO_2) emissions in 2018, with road transport accounting for three-quarters of this total (IEA, 2019).

Recent IC engines are characterised by more and more complex architecture to improve efficiency, without deteriorating power and torque performance and to comply with CO_2 emission specifications. Downsizing of IC engines has been recognised as an effective way to enhance engine efficiency and reduce CO_2 emissions. This strategy, however, may cause the onset of harmful autoignition during combustion, commonly known as engine knock (Kalghatgi, 2014).

It is evident that no other feature has directed the development of spark ignition (SI) IC engine technology as did the assurance of knock free operation. Research octane number (RON) and motor octane number (MON) are measured fuel properties indicating the fuel's resistance to auto-ignition. Fuels with higher octane ratings are able to resist knock in IC engines operating at higher compression ratios (CR).

The development of engine technology was therefore closely followed by the development of fuel technology. From a fuel producers point of view, two often conflicting challenges must be satisfied. Firstly, to meet internationally recognised or national fuel specifications and secondly to do so in the most economical manner possible.

Since the development of the first fuel specification and due to the modern trend of downsizing, the octane rating of a fuel is probably the single largest challenge addressed by fuel producers. The phase-out of heavy metal fuel additives for octane enhancement has forced fuel producers to adhere to new specifications and to invest in new technologies to produce higher octane fuels.

South Africa is on the brink of adopting significantly tighter national fuel specifications known as Clean Fuels II (CF2). While these specifications promise notably cleaner road transport scenarios, they pose a great investment challenge for fuel producers in South Africa. Fuel producers are thus now actively pursuing the transition to CF2 specification fuel products. The octane upgrading capabilities of a petrol product is directly affected by the CF2 transition with certain high octane blend ingredients now being restricted.

Although octane measurement has existed for many years, it is surprisingly poorly understood at the fundamental level. This project made use of Stellenbosch University's Cooperative Fuel Research (CFR) engine that is one-of-a-kind in South Africa. Uniqueness lies in the CFR engine's capabilities to now test high octane (RON $>$ 100) and oxygenated ($>$ 25 % by volume) fuels.

This CFR engine was used to study synergistic and antagonistic octane blending behaviours of common hydrocarbon and oxygenate molecular classes and octane boosting additives. Findings will provide fundamental know-how to enable Sasol to develop mathematical modelling tools to solve CF2 octane challenges. Successful execution of this project will also allow for accurate and credible high octane and oxygenated fuels research at Stellenbosch University, which was previously not possible.

Sasol (Pty) Ltd is the project sponsor. Sasol is an international integrated chemicals and energy company made up of many operating business units. This project is engaged with the Energy Technology team, specifically the Sasol Fuels Application Center (SFAC). The SFAC is involved in ongoing fuel research and provides support to Sasol's production plants.

1.2 Motivation

This research was undertaken to characterise important non-linear blending behaviours of important chemical class components, which make up the SI fuel recipe. In most instances, the necessary data is not available at a fundamental level, except for binary blends of the primary reference fuels (PRF), which define the octane scale. In terms of refinery economics, accurately predicting the RON and MON of a full boiling range (FBR) petrol is highly dependent on this data, which is used in various octane predicting manners. Therefore,

carefully selected components representative of the common classes, found in petrol, were experimentally tested to acquire octane blending data previously not known or not investigated on a fundamental level, using neat high purity fuel components.

This study falls under a multi-faceted research project that has been pursued by the SFAC over several years, and of which this thesis forms an integral part. Stemming from this, Bergenthuin (2018) modified Stellenbosch University's CFR engine to provide octane testing of high octane and oxygenated fuels. These capabilities, together with this project, will potentially enable optimisation opportunities within a refinery without compromising the quality or production of its fuels. Not only will this research assist refinery efforts, but primarily contribute valuable information in this research field.

1.3 Hypothesis

1.3.1 Foundational assumption

This study's foundational assumption is that each petrol component class behave similarly with respect to octane rating.

1.3.2 Hypothesis

The foundational hypothesis of this study is that non-linearities do exist in octane blending between binary combinations of common fuel components of the SI fuel recipe and more than one non-linearity (synergism and antagonism) can exist in such a blend combination.

1.4 Objectives

This project aims to characterise the various synergistic and antagonistic petrol component chemical class effects and octane additive effects on octane blending behaviour. This will be achieved via experimental blending and octane testing of pure fuel and additive components selected to represent the main component classes of petrol and promising octane boosting compounds, respectively. The project further aims to distil insights from the obtained data set regarding the non-linear octane blending responses for use in follow-on modelling or experiments.

The objectives set out for successful completion of the project are therefore:

1. Perform a comprehensive literature review to develop the necessary un-

derstanding and knowledge behind the projects scope and to inform experimental design.

2. Design an experimental testing matrix based on chosen variables and given constraints.
3. Recommission Stellenbosch University's CFR engine ensuring octane measurements are up to the accepted standards.
4. Perform blending and engine experiments based on experimental testing matrix.
5. Extract and post process the raw experimental data for interpretation.
6. Provide useful insight into the newly characterised non-linearities between chemical class components.
7. Provide useful insight and suggest mathematical functions suitable for modelling the non-linear octane blending behaviour results.
8. Discuss any limitations and/or recommendations for future research.

1.5 Report overview

This report documents and describes the methods used to characterise the non-linear octane blending behaviour between binary combinations of carefully selected chemical class components.

Chapter 2 provides a literature review used to gain an understanding of the existing research and arguments relevant in this research field. It also lays down important literature for the understanding and interpretation of the project results and conclusions.

Chapter 3 discusses the experimental methodologies which were implemented to meet the project's aim and objectives. The project's experimental results are then presented in Chapter 4. Chapter 5 focuses on optimising and improving the predictive capabilities of a well known mathematical octane prediction model.

Chapter 6 is an in-depth discussion of the study's results and findings. Chapter 7 concludes this report and Chapter 8 provides recommendations for future research.

Chapter 2

Literature Review

2.1 Knock in spark ignition (SI) engines

2.1.1 Introduction to knock

Combustion in spark ignition (SI) engines can be divided into normal and abnormal combustion, where normal combustion is desired for optimal operation. During normal combustion the air-fuel gas mixture is ignited by a spark, after which the flame front propagates from the spark outwards, completely consuming the gas mixture in a controlled manner. Conversely, autoignition is an abnormal combustion phenomenon, which can cause harmful damage in SI engines (Cengel, 2015).

Autoignition is the spontaneous ignition and the resulting rapid reaction of a portion or all of the gas mixture without an external ignition source. In SI engines the term 'knock' is traditionally identified by a sharp metallic ringing noise caused by this rapid autoignition of the unburnt air-fuel mixture, also known as the end-gas (Heywood, 1988).

In the early stages of SI engine development pre-ignition was typically confused with autoignition and vice versa. Pre-ignition is another abnormal combustion phenomenon, specifically a surface ignition phenomenon, where the air-fuel mixture is ignited by a hot spot on the combustion chamber wall. For example, a hot spot caused by an overheating spark plug or glowing combustion chamber deposits (Heywood, 1988).

Figure 2.1 distinguishes between typical pressure traces for normal, knocking and pre-ignition combustion.

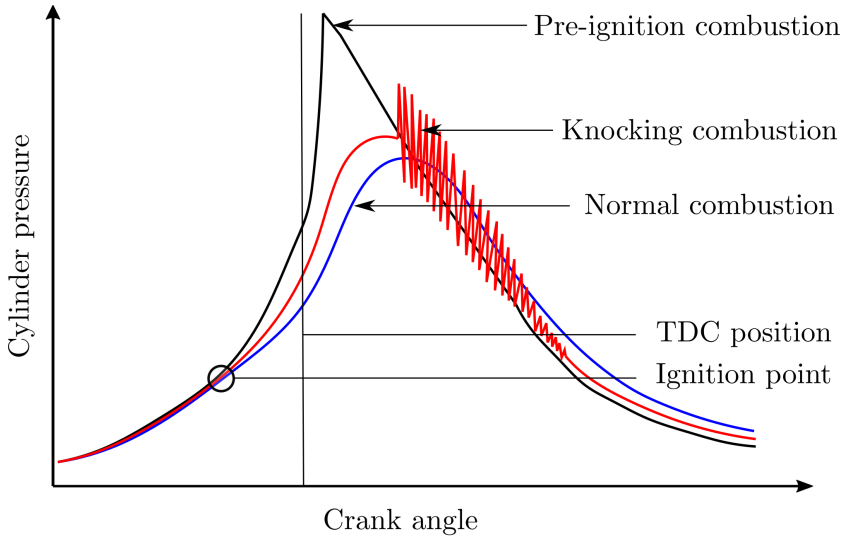

Figure 2.1: Pressure traces illustrating normal, knocking and pre-ignition combustion. Adapted from (Kalghatgi, 2014).

Some of the earliest research into autoignition by Hopkinson at Cambridge University, showed that knock is not a pre-ignition phenomenon, but conclusively a pressure disturbance that occurred after ignition by the spark plug discharge. Knock is now universally accepted to be a consequence of autoignition in the unburnt end-gas ahead of the propagating spark-ignited flame front (Miller and Fisk, 1987). It is also important to understand that although knock is caused by the autoignition of the end-gas, autoignition will not always lead to knock (Konig and Sheppard, 1990).

Throughout the history of SI engines, knock has placed an upper limit on the maximum allowable CR of the engine. To increase the thermodynamic efficiency of a SI engine, the CR must be increased. However, increasing the CR also increases the end-gas temperature and pressure. At higher temperatures and pressures induced by higher CRs or charge boosting, the engine is more prone to knock.

During knocking conditions, the autoignition of the unburnt end-gas creates localised pressure spikes and an increase in combustion chamber heat transfer, both of which can cause harmful damage to the engine (Kalghatgi, 2014).

The onset of knock in SI engines effectively limits the CR and thus the thermodynamic efficiency. Knock is an important consideration in SI engines as it is an inherent design constraint, limiting the efficiency and power of the engine.

2.1.2 The octane rating scale

A fuel's tendency to knock depends on engine design and the operating conditions which influence the end-gas temperature and pressures. However, for a given engine configuration, the presence or absence of knock depends primarily on the anti-knock quality of the fuel (Heywood, 1988).

To compare the quality of different fuel blends, a practical measure of a fuel's resistance to knock is used. This measure is defined by the octane number (ON) scale. It is traditionally measured by the RON and MON of the fuel. The tests are conducted in the single cylinder Cooperative Fuels Research (CFR) variable CR engine, in strict accordance with the procedures set in the American Society for Testing and Materials (ASTM).

The ASTM standards are continuously revised and updated. The ASTM standards adopted in this project are the D2699-19 ASTM (2019*a*) and D2700-19 ASTM (2019*b*) standards, where the number following the designation is the year of original adoption. Please note that from this point on these standards will be referred to as 'D2966' for RON and 'D2700' for MON.

Originally proposed by Edgar (1927), the extremes of the octane number (ON) scale are based on the resistance to knock of the two paraffins n-heptane and isooctane defined by ONs of zero and 100 respectively. Volumetric blends of these two primary components are known as primary reference fuels (PRFs) and define the octane scales for RON and MON. For example, a blend of 95 percent by volume isooctane and five percent by volume n-heptane is assigned the ON of 95 (PRF95) on both RON and MON scales. By definition, these two PRFs blend perfectly linearly.

The numerical difference between RON and MON is defined as the octane sensitivity ($OS = RON - MON$). The RON and MON values of the PRFs are equal, therefore, the OS of a PRF blend equates to zero. For non-PRFs, OS is non-zero and the larger the value the more sensitive the fuel is to operating conditions, specifically pressure (Blackmore, 1977).

The marketing and manufacture of fuels in the transport industry are immensely influenced by the fuel's requirements to meet specific RON and MON specifications. This is why the ON of practical fuels is amongst its most important quality properties (Kalghatgi, 2014).

2.1.3 Basic chemistry of SI engine fuels

The autoignition chemistry of SI fuels affects engine performance and emissions. SI fuels are complex mixtures of hydrocarbons that vary by class and size (Kalghatgi and Stone, 2018).

The main classes of hydrocarbons found in petrol are paraffins (alkanes), olefins (alkenes), naphthenes (cycloalkanes) and aromatics. The ON of hydrocarbons varies greatly with chemical structure. RON and MON values of pure hydrocarbons decrease in the following order: aromatics, isoalkanes (isoparaffins), olefins, naphthenes (cycloparaffins) and n-alkanes (n-paraffins) (Anderson *et al.*, 2010). The main classes of oxygenates used in SI fuels are alcohols and ethers. SI fuels also contain sulfur and nitrogen compounds and traces of metal compounds.

It is common for fuels to contain additives, which are chemicals added in small quantities to improve engine efficiency and power and/or correct a fuel deficiency (Kalghatgi, 2014). Some knowledge of the hydrocarbon and oxygenate classes and other fuel additives is necessary to understand their effects on the likelihood of knock within the scope of this study.

The anti-knock properties of hydrocarbon molecules decrease with the increase of carbon atoms. The rate of autoignition is dependent on the rate of removal of hydrogen atoms during the combustion process, therefore, autoignition depends on the strength of the carbon-hydrogen (C-H) bonds within the molecule structure. In addition, Ronney (2013) concluded that C-H bonds are stronger when fewer carbon-carbon (C-C) bonds exist within the hydrocarbon molecule. Stronger C-H bonds decrease the reaction rates and, therefore, the likelihood of engine knock.

A branched molecule (Figure 2.2a) is shown to have higher knock resistance than straight chain molecules (Figure 2.2b) with equal number of carbon atoms (Heywood, 1988).

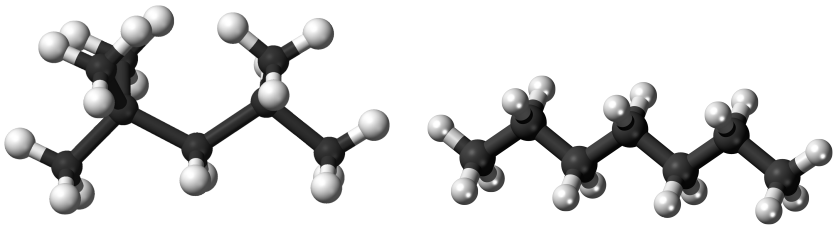

(a) (b)

Figure 2.2: A branched molecule (a) with higher knock resistance than a straight chain molecule (b).

It is also important to highlight the concept of a stable or unstable molecule or fuel. In SI chemistry terms, a fuel is understood to be stable or unstable in relation to its propensity to form deposits and gums. A stable fuel is more resistant to autoignition than an unstable fuel.

2.1.4 Component class SI chemistry

Paraffins (alkanes) are single bonded open chain saturated hydrocarbon molecules. Increasing the length of a paraffin chain increases the tendency of knocking (Figure 2.2b), therefore compacting the molecular structure (branching shown in Figure 2.2a) shortens the chain length and decreases the tendency of engine knock. Using groups of methyl molecules can also decrease the knocking tendency (Richards, 2014).

Olefins (alkenes) are unsaturated hydrocarbons (contain at least one double bond between two carbon atoms) and generally have good antiknock behaviour. Olefins do however increase deposit formation in fuel injectors and are thermally unstable. The maximum allowable olefin content in Europe is set to 18 % by volume (Kalghatgi and Stone, 2018).

Naphthenes (cycloparaffins) are characterized by having one or more rings of saturated carbon atoms. Naphthenes are an important component of the petroleum refinery process and like paraffins are very stable. However, according to Heywood (1988), naphthenes have significantly greater knocking

tendency than a similarly sized aromatic molecule. Therefore careful control of naphthenes in the petrol recipe is crucial (Richards, 2014).

The building block for an aromatic hydrocarbon is the benzene ring (C_6H_6) and examples include toluene and xylene. The benzene ring is very stable and accommodates additional CH_2 groups to give the general molecular formula C_nH_{2n-2}. This molecular structure contributes significantly to a fuel's anti-knock quality and has a high volumetric energy content. Lowering aromatic content has also been shown to reduce toxic benzene emissions in vehicle exhausts (Heywood, 1988; Kalghatgi and Stone, 2018). However, heavy aromatics can also lead to increased combustion chamber deposits. Aromatics also produce more CO_2 for a given energy content because of their higher C-H ratios. In both Europe and the United States, the maximum allowable aromatic content in petrol is set to 35 % by volume. However, the maximum allowable benzene levels in Europe are controlled at 1 % by volume (Kalghatgi and Stone, 2018).

The phase-out of octane enhancing, heavy metal fuel additives such as tetra-ethyl lead (TEL), forced fuel producers to invest in new technologies to produce fuels with intrinsically higher ONs as well as reduce environmental impacts. Oxygenates such as ethanol (alcohol) and tertiary amyl methyl ether (TAME) have excellent anti-knock qualities and are used extensively as petrol additive components.

An oxygenate contains oxygen as part of its molecular structure, and there are many oxygenates commonly used as fuel additives. Ethanol is produced from biosources and is attractive for reasons of energy security due to it possibly having a lower greenhouse gas footprint. Ethanol made from sugarcane is used extensively in Brazil and is also increasingly used in the United States, with an allowable volume percentage of 15 % from the year 2010 (Kalghatgi and Stone, 2018). Figure 2.3 shows the molecular structure of ethanol, containing oxygen.

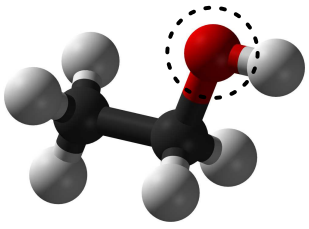

Figure 2.3: Ethanol molecule, with additional oxygen atom (circled).

The difficulty in using oxygenates is the component's lower volumetric energy content and the effect on evaporative emissions and driveability. Due to this, there are various ASTM specified CFR modifications used to satisfy the octane measurement challenges of measuring high oxygenated and octane fuels. These studies and modifications are discussed later in Chapter 3.

The use of ethanol blended into petrol surrogates has been studied extensively in literature to better understand various non-linear octane blending behaviours, whilst improving a fuel's anti-knock quality (Foong *et al.*, 2014; Yuan, 2018). In general, the use of ethanol is increasing across the world.

2.2 Octane measurement

The methods, experimental equipment and testing materials have remained relatively unchanged since 1939. These methods are still used today as the industry standard for octane research and more importantly providing octane quality control parameters for SI fuels.

2.2.1 Knock measurement system

The first quantification of knock was accomplished using the bouncing pin, named the Midgley design, after Thomas Midgley Jnr (Midgley Jr and Boyd, 1922). By 1948 the measurement of RON and MON was adopted by the ASTM. The manual contained a description of the bouncing pin based on the Midgley design and detailed instructions for its usage (ASTM, 1959).

The bouncing pin was used as the standardised knock intensity (KI) measuring device until 1970 when it was replaced by an electronic knock measurement system comprising of a magnetostrictive D1-pickup, which is flush-mounted in the combustion chamber, a detonation meter and a knockmeter. The sensor's signal is conditioned by the 501T detonation meter, which applies a low pass filter and time averages the signal.

A knockmeter and detonation meter are shown in Figure 2.4.

(a) (b)

Figure 2.4: Knock meter (a) and detonation meter (b).

A knockmeter has divisions from zero to 100 to show the resulting KI when the CFR engine is running. As the KI increases so does the analogue meter needle. A value of 50 ± 2 divisions was chosen as the standard KI value. The model 501T detonation meter has various calibration settings. The calibration techniques of the detonation meter can be found in either of the ASTM standards. This electronic measurement system is used today, in accordance with the ASTM standards, and is present on the CFR engine at Stellenbosch University.

Swarts *et al.* (2004, 2005) detected various anomalies in the ASTM RON and MON tests, with one result showing that the in-cylinder pressure oscillations were highly dependent on the fuel composition. The work by Hoth *et al.* (2019) and Rockstroh *et al.* (2018) expanded on these findings, showing further insight. Mittal and Heywood (2008, 2010) proposed altering the CFR engine operating conditions to better fit modern engines.

Although these studies have shown that the ASTM specified knock measuring system does not correlate well with accurate measurements of knock, the ASTM standards and CFR engine used to measure RON and MON are standardised methods accepted internationally throughout the fuel industry. It is therefore suggested to follow these standards to contribute to this already well established field with valuable data in alignment with the standardised methods.

2.2.2 Octane rating equipment and conditions

Stellenbosch University's CFR engine is a CFR F1/F2 Octane engine. The CFR F1/F2 Octane engine is the internationally accepted standard for determining the RON and MON of SI fuels, with a measurement range of 40 to 120 ON. Other CFR engines include the CFR F5 Cetane and the CFR F4 Aviation fuel rating units. Throughout this report, the CFR F1/F2 Octane engine is simply referred to as 'CFR' or 'CFR engine'.

The CFR engine is a standardised single cylinder, four-stroke, naturally aspirated and carburettor fuelled SI engine with a variable CR. Engine knock can be induced by adjusting the CR within the adjustable range of 4:1 to 18:1. The operating conditions applicable to RON and MON octane rating conditions are given in Table 2.1.

Table 2.1: Standard operating conditions for RON and MON.

Parameter	RON	MON
Engine speed	600 rpm ± 6 rpm	900 rpm ± 9 rpm
Oil temperature	57 °C ± 8 °C	57 °C ± 8 °C
Inlet air temperature (IAT)[a]	52 °C ± 1 °C	38 °C ± 2.8 °C
Intake mixture temperature (MIXT)[b]	Not controlled	149 °C ± 1 °C
Cylinder jacket coolant temperature	100 °C ± 1.5 °C	100 °C ± 1.5 °C
Spark timing	13° BTDC	14° to 26° BTDC
Air-fuel ratio (AFR)	Adjusted for maximum KI	Adjusted for maximum KI

[a,b] Adjustable within range specified in ASTM standards for TSF tuning.

It is clear that the operating conditions in Table 2.1 bear little similarity to those of modern downsized and boosted SI engines. Yates *et al.* (2005) confirms this by showing that the historical ASTM operating conditions were chosen to bracket the normal operating conditions of a carburettored engine.

There have been numerous studies to re-visit the ASTM specified conditions as the benchmark to certify the ON of fuels for modern non-carburettored, boosted and intercooled engines. Examples of these studies include those by Millo *et al.* (1995) and recently Mittal and Heywood (2008) and Mittal and Heywood (2010). However, as stated previously, this study will

follow the recognised standards closely and these studies will not be discussed here.

2.2.3 Octane index

The RON and MON values can be combined to provide further insight into a particular fuel's anti-knock characteristics. The anti-knock quality of a fuel at a given engine operating condition can be described by its octane index (OI), as shown in Equation 2.1.

$$OI = RON - K(OS) \tag{2.1}$$

The OI depends on the RON value, the OS ($RON - MON$) and a K value. The higher the OI, the better the anti-knock quality of the fuel. The K value is defined as zero for RON and one for MON. However, as shown by Kalghatgi (2001*a*) the K value is dependent on engine operating conditions, and in some cases, can be negative. For example, for a given RON and negative K, a sensitive fuel (lower MON) has better anti-knock qualities using Equation 2.1.

Kalghatgi (2001*a*) showed that K decreases as the engine approaches the knocking limit, i.e., as the octane requirements increase. Kalghatgi (2001*a*) also showed that in terms of the end gas properties, K decreases as the temperature decreases for a given pressure. Kalghatgi (2001*b*) concludes that modern Japanese and European SI engines prefer fuels of higher sensitivity with high RON values. Anderson *et al.* (2012) also states that RON is the better predictor of knock potential than MON, in modern engines.

Boot *et al.* (2017) studied the relationship between OS and K values for isooctane, toluene and 2-methylheptane. It was concluded that in modern engines, fuels with high OS outperform their less sensitive counterparts on the OI scale, independent of RON value.

Yates *et al.* (2005) provides an attractive method for graphically displaying the relationships between OS, knock-limited test data and high and low speed knocking conditions. Using this graphical approach, Yates *et al.* (2005) presented the following:

1. A fuel with high sensitivity has an increased potential for knocking at high engine speeds with a carburettored engine.
2. High speed knocking is less likely in modern fuel-injected engines equipped with either a turbo- or super-charger and an intercooler.

3. It is very likely that modern forced induction engines would operate well on fuels with high sensitivities. This was also intimated by Kalghatgi (2001*b*).

4. Paraffinic fuels are more likely to knock at low engine speeds.

Leppard (1990) investigated the chemical origins of OS by studying different chemical component classes. For paraffins, there is a two-stage ignition process: a low temperature heat release of the air-fuel mixture followed by a negative temperature coefficient (NTC) region, where the reaction rates become inversely proportional to temperature. This facet has been used to improve the understanding of the K value in Equation 2.1 and for improving various empirical octane prediction models used in refineries.

Using these findings, important insights can be formulated by studying the OS between the various blends studied in this project. For example, the OS of a test sample may change over various blend ratios, exposing where this particular fuel may be more beneficial to the operation of say a modern, highly boosted and downsized engine versus a naturally aspirated and carburettor fuelled engine.

2.2.4 Octane measuring procedures

The octane number of a fuel is determined using the CFR engine within a test cell laboratory. The CFRs engine speed is kept constant by a dynamometer. The specific engine operating conditions can be found in Table 2.1.

The D2699 and D2700 standards were designed to simulate different driving conditions. The MON method is accepted as the more severe engine operating condition. The MON method introduces mixture heating with the addition of the MON pipe. The MON pipe is fitted between the carburettor and intake port of the cylinder head. Additional heaters are used in conjunction with the MON pipe to control the air-fuel mixture temperatures (MIXT). The ASTM standards list four acceptable octane measurement procedures for measuring both RON and MON. A detailed description of each can be found in the relevant standard. The four ASTM procedures are listed here:

1. Procedure A: Bracketing-Equilibrium Fuel Level.

2. Procedure B: Bracketing-Dynamic Fuel Level.

3. Procedure C: Compression Ratio.

4. Procedure D: Bracketing-OA.

Using Stellenbosch University's CFR engine, Procedure D cannot be used. Procedure D requires a newer CFR engine with automated CR adjustments with additional hardware and software. Both Procedure A and Procedure B can be used as bracketing methods, however, Procedure A was adopted in this study due to its time efficiency. Procedure A will be referred to as the 'bracketing method' from this point on in the report.

During an engine experiment, a liquid fuel test sample is introduced through the selected fuel reservoir. The CR is estimated and then adjusted, together with the air-fuel ratio (AFR), to obtain standard KI. Once standard KI is obtained, an ON can be calculated using the reference tables found in the ASTM standards to relate a CR to an ON. It is common practice to perform further bracketing tests where two PRFs are blended (one PRF of higher ON and one PRF of lower ON) and measured in the CFR engine. If the PRFs bracket the test sample within an acceptable tolerance, the test samples ON can be linearly interpolated. This ensures that the engine measurements are further scrutinised to meet the measurement accuracies specified in the ASTM standards.

Specific to the CR procedure (Procedure C), is the generation of a calibration curve (CC), relating CR to an ON. The CC is obtained by running the CFR engine at the same operating conditions on different PRFs spanning the measurable ON range. A CC is generated for both RON and MON. According to the ASTM standards, a CC is unique to a particular CFR engine and must be verified by the fit-for-use TSF tests. The CC essentially eliminates the use of the ASTM reference tables and brackets an ON by interpolation between points on the CC.

Kalghatgi *et al.* (2014) used the CR procedure in conjunction with a CC to successfully measure the RON values of various PRF and TSF fuels between an ON of 50 and 100. RON tests were performed using an ASTM specified CFR engine and followed the D2699 ASTM standards. The RON results were verified using a second single-cylinder research engine, to compare the KI of the fuel test samples.

There are other distinguished research by Swarts (2006), Viljoen (2009), Anderson *et al.* (2012), Foong *et al.* (2014) and recently Yuan (2018), who also used an ASTM specified CFR engine and a CC. These studies will be discussed throughout this report.

In summary, the CR procedure is used to initially measure the ON using the ASTM reference tables and a CC. After which, further bracketing tests are performed to bracket the test sample within a specified tolerance.

2.3 Octane properties of SI fuels

2.3.1 Overview

Octane numbers are routinely measured and numerically modelled in refineries worldwide. Although both processes are challenging due to experimental complexities and numerical non-linearities, it is desirable to experimentally characterise the octane blending behaviours of different chemical classes. This can potentially provide insights and data foundation for the formulation and improvement of numerical octane prediction models.

The chemical classes of the petrol recipe components behave differently with respect to octane blending, with synergistic and antagonistic non-linear effects depending on compositions of the component and the matrix into which it is blended (Scott, 1958). Synergistic blending is a measured ON that is higher than that obtained by linear interpolation from that of its pure constituents, whilst antagonistic blending is a measured ON that is lower than that obtained by linear interpolation from that of its pure constituents (Foong et al, 2014).

For example, with reference to Figure 2.5, using the analogy of two pharmaceutical drugs: if the two drugs (Drug A and Drug B) work together to create an effect greater than the sum of their individual effects (straight line), then this is known as synergistic blending. The opposite is true for antagonistic blending. There is also a possibility that a combination of the two blending behaviours can exist together.

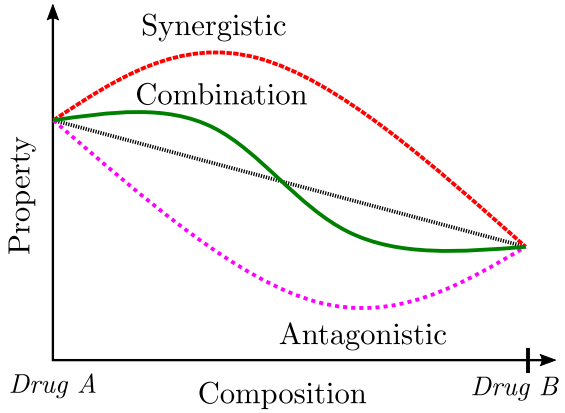

Figure 2.5: Illustrative example showing linear and non-linear blending.

2.3.2 Octane measurements of pure components

The American Petroleum Institute (API) data represents one of the most reputable sources of octane data associated to SI fuels and was generated during the API Project 45 (American Petroleum Institute, 1957). It describes individual molecular characterisations and it includes the RON and MON measurements of pure hydrocarbon compounds as well as their ONs when blended with 20 % by volume ratio with 80 % PRF60.

Research by Anderson *et al.* (2010), Anderson *et al.* (2012), Foong *et al.* (2014), Kalghatgi *et al.* (2014), Yuan (2018) and da Silva Jr *et al.* (2019) are valuable in the field of octane blending behaviours. These studies provide RON and MON data for various pure components and binary component blends. This data is valuable to this research: the components used in these studies were amongst the selected components in this study and measurements were performed using a CFR engine in strict accordance with the ASTM standards.

2.3.3 Octane measurements of blending behaviours

Covering all distinguished research in the field of octane blending behaviours was beyond the scope of this text. The following criteria were used to select any relevant literature in support of this research:

1. Octane measurements must be performed using a CFR octane rating engine, in strict accordance with the ASTM standards.
2. Focus was placed on previous research, which used similar fuel components selected in this project.

Anderson *et al.* (2010) investigated the applicability of a molar based ON blending model using the API data and various other data found from literature. RON and MON data were used to compare various volumetric and molar concentrations of ethanol and methanol in order to show that molar blending values are independent of the base petrol's ON. Results showed that there was a linear increase in RON and MON values with alcohol content.

However, Anderson *et al.* (2010) found little difference when comparing volumetric and molar composition blending of the ethers methyl tert-butyl ether (MTBE), ethyl tert-butyl ether (ETBE) and TAME. This was because the molecular weights of the alcohol and ether components were closer to the base petrol's hydrocarbon molecular weights, causing the molar and volumetric concentrations to be similar. As a result, there is little difference in the octane

predictions for these compounds, using a volumetric or molar concentration basis.

Routed from this study, Anderson *et al.* (2012) documents the RONs and MONs for a matrix of ethanol-petrol blends in order to support and evaluate the findings of the previously introduced linear molar octane blending model by Anderson *et al.* (2010).

Octane measurements were performed using two independent CFR engines from two separate laboratories, both modified for satisfying the RON and MON measurement challenges of measuring ethanol-petrol blends found in Anderson *et al.* (2010). The one engine was equipped with adjustable orifice fuel jets and the other using automation and digital controls intended to increase accuracy and reproducibility. Up to 75 % ethanol was blended into four well established and characterised blendstocks to formulate the matrix of blends to be tested.

Conversion from volumetric to molar concentration was performed and the results were compared to draw the following conclusions: it was found that both RON and MON results of the ethanol petrol blends displayed well known non-linear behaviours with volumetric ethanol concentrations. However, when plotted using molar ethanol concentrations, most non-linearities were not present. Therefore Anderson *et al.* (2012) showed that the ONs could be interpolated linearly when plotted on a molar basis.

This study confirms that different components from the petrol recipe do behave differently with respect to octane blending behaviour, however, in terms of refinery operations, using a molar basis to linearly interpolate ON estimations is not practical due to the fact that a FBR fuel has many constituents with unknown molecular information. Therefore, this method would be very difficult to use in practice.

Foong *et al.* (2014) studied the RON and MON of ethanol blended with production petrol, four petrol surrogates, n-heptane, isooctane and toluene. The RON and MON values were also measured using a standardised CFR engine and tests were performed according to the ASTM D2699 and D2700 standards. The ethanol volume concentration was varied from 0 to 100 percent to extract any synergistic and/or antagonistic blending behaviours that might be present.

Initially, Foong *et al.* (2014) found that ethanol blended non-linearly in Australian and US production petrol. The slight synergisms were attributed to the varying petrol compositions, including notably different aromatic content but similar RON and MONs. This prompted a systematic study of the blending behaviours of ethanol blended into four petrol surrogates, isooctane, n-heptane

and toluene. One PRF blend and three different toluene reference fuels (TRF) blends were selected as the petrol surrogates. These were, PRF91 (RON and MON both equal to 91), and PRF91 blended with 15, 30 and 45 percent toluene to give TRF91-15, TRF91-30 and TRF91-45, respectively.

Both isooctane, n-heptane and their PRF blends were found to blend synergistically with ethanol, whilst toluene was found to blend antagonistically with ethanol. The RON octane blending results are shown in Figure 2.6. Similar binary blending relationships were concluded for the MON results (Foong *et al.*, 2014).

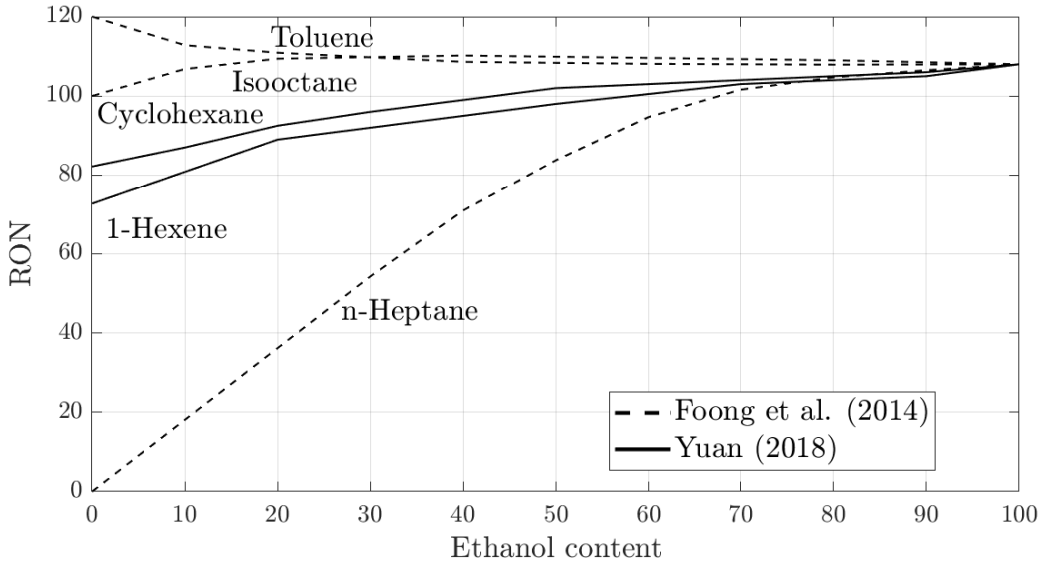

Figure 2.6: Measured RONs of ethanol/isooctane, ethanol/n-heptane and ethanol/toluene by Foong *et al.* (2014).

Consistent with these trends, Foong *et al.* (2014) found that a progressive increase in toluene content in the TRFs, with a constant RON, resulted in increasingly linear ethanol-TRF blending. The TRF15 (TRF and 15 % ethanol) exhibited the greatest synergism in RONs with ethanol, followed by TRF30 and lastly TRF45. Therefore, Foong *et al.* (2014) showed that the antagonism of ethanol's blending with toluene acts against its synergism with isooctane and n-heptane, and more broadly suggests that the antagonism of ethanol's blending with aromatics may act against its synergism with paraffins.

Yuan (2018) studied the blending interactions between TRFs, 1-hexene and cyclohexane blended into ethanol for developing a five component petrol surro-

gate. The non-linear synergistic and antagonistic blending observed between 1-hexene/ethanol and cyclohexane/ethanol binary blends are of significant value to this study and are also plotted in Figure 2.6.

These studies show that a given octane number can be achieved with lower aromatic and alcohol content, which could enable refineries to exploit the synergism of ethanol and paraffins to make more effective use of ethanol as an alcohol in their blends. This could lead to environmental and economic benefits for refineries.

There is little octane blending data for TAME. Botha *et al.* (2002) studied the blending interactions between 95/5 Sasol Fuel Alcohol (SFA - 95 % ethanol and 5 % propanol) and the ethers MTBE and TAME. A synergistic blending behaviour was found between ethanol and TAME. Even though SFA was used and not ethanol, this is an important finding for this project, because it specifically targets the non-linear blending behaviours of an alcohol blended into the ether TAME.

2.4 Octane prediction modelling

2.4.1 Overview

The significant goal of predicting the octane of a fuel from fundamental autoignition chemistries has remained an elusive target challenging the efforts of researchers over the past few decades (Yates *et al.*, 2005). During this period, valuable data and insight have been gained and it is possible to identify the following general approaches used to predict octane:

1. Chemical kinetic and empirical prediction models.
2. Laboratory experiments involving a variety of engine and fuel configurations to correlate engine performance and operating conditions to ON.
3. Road experiments to characterise vehicle performance against a fuel's octane rating.
4. Experimental autoignition studies, which typically include devices such as rapid compression machines (RCMs), shock tubes, constant volume vessels, jet-stirred reactors and many others.

Covering all available models is beyond the scope of this study, however, it is important to distinguish between the different approaches. This study primarily focuses on laboratory experiments and well established empirical prediction models.

2.4.2 Empirical octane blending models

It is no longer accepted that a linear-by-volume (LBV) calculation (see Figure 2.5) is accurate enough for estimating the ON of FBR petrol blends (Stratiev *et al.*, 2017). Models that include non-linear blending behaviours of typical petrol blends have been described in numerous studies with varying success.

The Stewart model is a good example of such a study and is based on the measured ONs of the separate petrol component streams and their volumetric olefin content (Stewart, 1959). The Stewart model is given by Equation 2.2.

$$ON D_{\text{mix}} = \frac{\sum_i V_{\text{i}} D_{\text{i}} (R_{\text{i}} + C P_{\text{i}})}{\sum_i V_{\text{i}} D_{\text{i}}} \tag{2.2}$$

Where, V_i is the volume of component i added to the blend, P_i is the olefin difference, $P_{\text{i}} = U_{\text{i}} - U_{\text{mix}}$, in volume percentage, with U_{mix} the LBV olefin content of the blend and U_i the olefin content of component i. D_i is the weighting factor given by Equation 2.3.

$$D_{\text{i}} = \frac{AP_{\text{i}}}{1 - e^{(\text{-AP}_{\text{i}})}} \tag{2.3}$$

Both A and C are regression constants and D_i and R_i is the octane number, either RON or MON depending on the desired prediction.

Sasol has used this model for many years with acceptable accuracy for olefinic fuels such as those produced from synthetic petrol as is being manufactured at the CTL complex in Secunda (Viljoen, 2009). Since the model classifies aromatic and paraffinic volumetric contents in one term (non-olefins), it is clear that the Stewart model will not be accurate under all circumstances, for example, fuels with high alcohol content. It is also one of the oldest models and thus might not be suitable to SI fuels being manufactured today.

The Stewart model has been extended by other researchers such as Healy *et al.* (1959). Named the Ethyl model, the non-linearities are modelled by the fuel sensitivity, olefin content and an additional term for aromatic contents (Healy *et al.*, 1959). The Ethyl model is given by Equations 2.4 and 2.5.

$$RON = \overline{r} + a_1(\overline{rj} - \overline{r}\,\overline{j}) + a_2(\overline{O^2} - \overline{O}^2) + a_3(\overline{A^2} - \overline{A}^2) \tag{2.4}$$

$$MON = \overline{m} + b_1(\overline{mj} - \overline{m}\overline{j}) + b_2(\overline{O^2} - \overline{O}^2) + b_3(\frac{\overline{A^2} - \overline{A}^2}{100})^2 \qquad (2.5)$$

Where, a and b are the predetermined Ethyl coefficients, r and m are the RON and MON values of each component in the blend, respectively, j is the sensitivity of each component, O is the olefin content in percent by volume and A is the aromatic content in percent by volume. The volumetric average of a variable is shown by $\overline{variable}$.

The Stewart and Ethyl models were compared by Viljoen (2009) by applying the models to 154 blends contained in the API data set. The standard error (SE) for RON and MON values using the Stewart model was 4.14 and 3.84 units, respectively. Whereas the Ethyl model RON SE was 4.36 and the MON 6.56 units. Viljoen (2009) concluded that these large errors in predictability is contributed to the fact that these models are not suitable for high purity components, such as the ones found in the API data.

Even though the Ethyl model distinguishes differences in hydrocarbon classes (olefin and aromatics) among petrol components, the model may produce unreasonable ONs (Twu and Coon, 1998). In order to overcome this Twu and Coon (1998) proposed an alternative binary interaction coefficient model (Twu and Coon model), utilising some of the concepts proposed by Morris (1975), and with coefficients for olefins, aromatics and saturates. The advantage of this model is that only three non-linear binary interaction parameters are required to obtain the correlation for blends with any ON.

Unfortunately, the Twu and Coon method requires a costly and complex blending study to determine and optimize the interaction coefficients. Added to this is the difficulty of forever changing fuel specifications, leading to the Twu and Coon model not being generally accepted.

Despite these disadvantages, the Twu and Coon model was adapted by Viljoen (2009), by optimising the interaction coefficients using distinctive insights of NTC characteristics of different fuel molecules. This empirical model containing NTC percentages had increased prediction accuracy with a SE for RON of 1.11 units and a SE for MON of 1.11 units.

There are many other empirical models for predicting the octane of FBR petrols, however, it was beyond the scope of this text to present all of them in this project (Daly *et al.*, 2016; AlRamadan *et al.*, 2016). It was also decided to focus specifically on the Stewart and Ethyl model to provide valuable insights into these models' prediction capabilities.

2.5 Literature review summary

The aim of this literature review was to gain an understanding of any existing research and arguments relevant to this field of research. It laid down important literature for the understanding and interpretation of the project's results, discussions and conclusions. Focus was placed on literature including octane measurements of similar components used in this study as well as the use of an ASTM specified CFR engine and methods.

The chapter began with presenting the fundamentals behind autoignition and knock in SI engines. It outlines how knock is quantified using the industry standard equipment and methods. It presents important autoignition chemistry behind SI engine fuels, with specific reference to their anti-knock characteristics. It also highlights important counter arguments found in literature, relating the ASTM specified octane rating equipment and conditions.

Distinguished research involving the study of octane numbers of single and multi-component fuel blends were presented. These studies played an important role in defining the project scope. OI is shown to be a valuable property, above and beyond the RON and MON values, to provide further insight into possible non-linear octane blending results.

Finally, important octane blending prediction models were presented and their advantages and disadvantages were also outlined.

Chapter 3

Experimental methodologies

3.1 Overview

This chapter details the experimental methodologies which were implemented to meet the project's aims and objectives. It begins by describing the CFR engine setup at Stellenbosch University. It includes the modifications present on the CFR engine with specific relevance to the ASTM standards and important literature sources. This chapter also describes the second experimental setup used in this project, namely, the gravimetric blending setup which was used for the blending of liquid fuel test samples. Lastly, this chapter describes the experimental phases and procedures which were implemented to obtain the raw experimental data.

Please also note that the blending ratios reported from this point on are blending ratios of percentage by volume, unless specified otherwise.

3.2 CFR engine setup

3.2.1 Overview

The engine experiments were carried out using Stellenbosch University's 1959 Waukesha CFR F1/F2 Octane rating engine, shown in Figure 3.1.

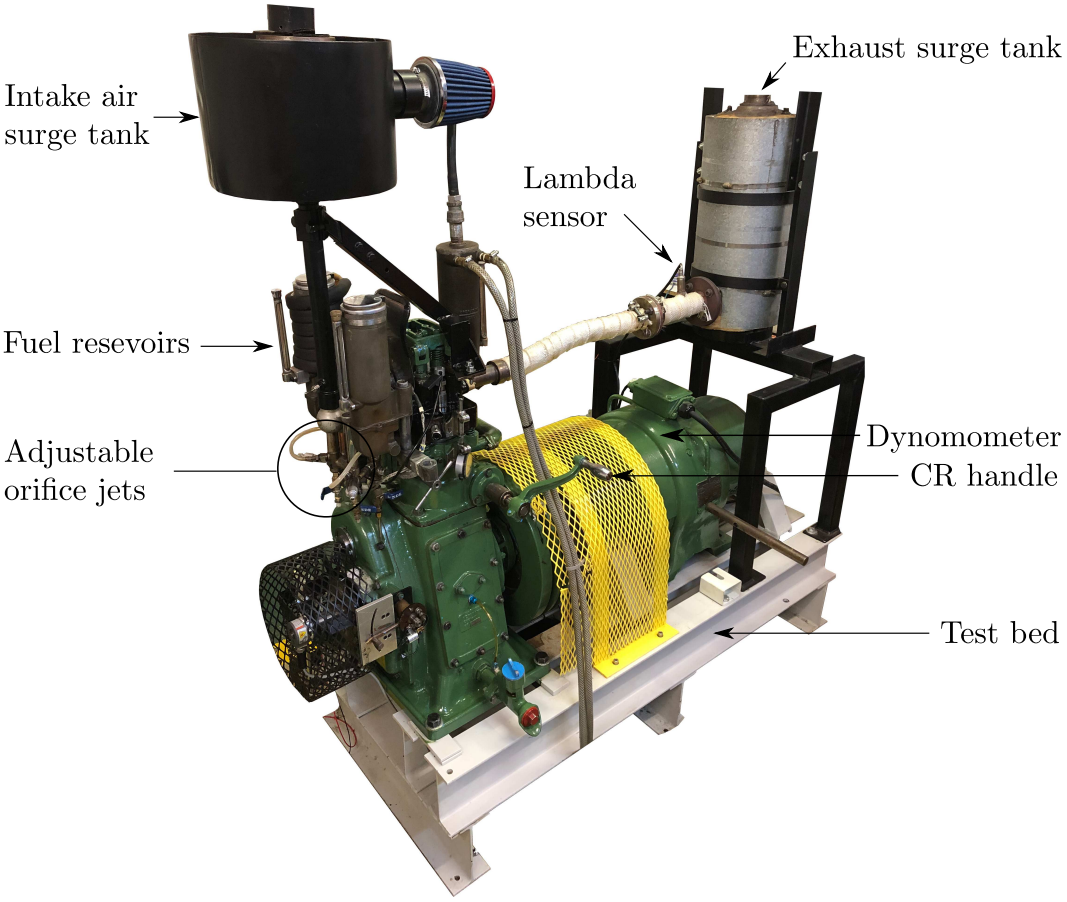

Figure 3.1: The CFR engine at Stellenbosch University.

A zoomed in view of the cylinder head is shown in Figure 3.2.

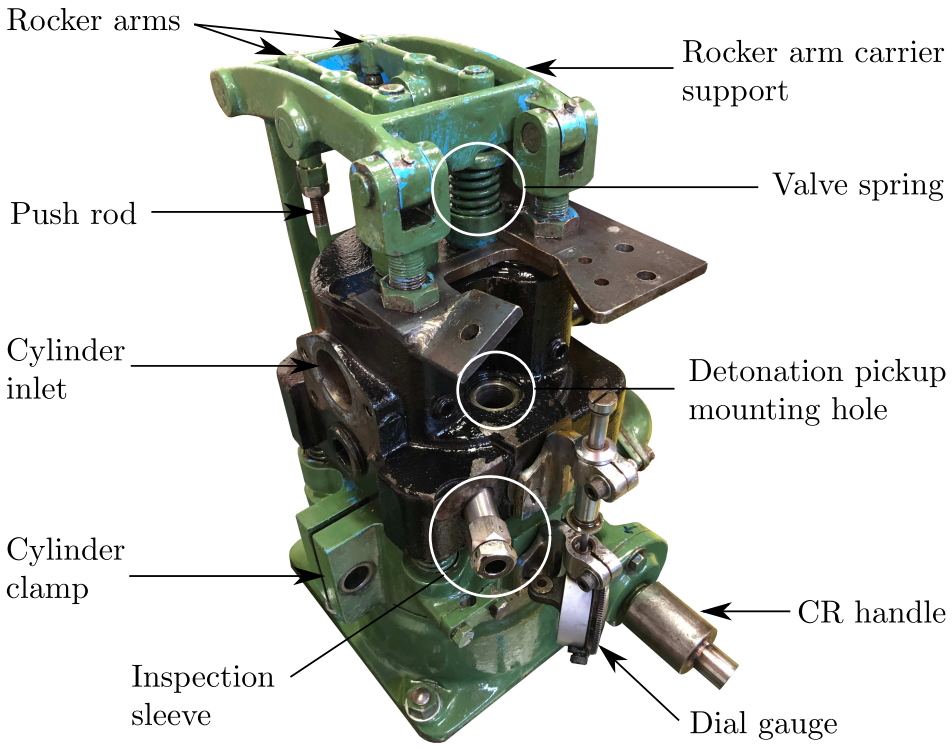

Figure 3.2: CFR engine cylinder head.

The engine operating conditions are controlled by the engine operator. The CFR engine's speed is kept constant by a dynamometer at 600 rpm for RON and 900 rpm for MON. During each experiment, a liquid fuel test sample is introduced through the selected fuel reservoir and mixed with air in the carburettor. The CR and AFR are adjusted according to the ASTM standards, to obtain a standard KI. Once standard KI is displayed on the knock meter, an ON can be calculated directly using the CC and ASTM reference tables.

During ON measurements the operator makes various adjustments. The CR is adjusted using the CR handle, in either a clockwise (decrease CR and KI) or anti-clockwise (increase CR and KI) direction. This adjustment is automatic on newer CFR engines. The inlet air (IAT), mixture (MIXT) and oil temperatures are controlled using auxiliary heaters. A number of additional temperatures are monitored, including coolant, oil, exhaust and ambient temperatures.

A dial micrometer, with an accuracy of 0.025 mm, is used to monitor CR adjustments. The AFR is finely tuned, to obtain maximum KI, using the adjustable orifice jet for each reservoir, together with a lambda sensor and ETAS lambda scanner. This is an improved modification over the standard AFR adjustment method of changing the fuel bowl height. All details of the instrumented CFR engine and auxiliary equipment are listed in Appendix A.

Recent research using this particular CFR engine included research projects by Swarts (2006) and Bergenthuin (2018). Swarts (2006) modified the engine to include horizontal line-of-sight optical access into the top of the cylinder via two inspection sleeves to accommodate in-cylinder pressure measurements. Bergenthuin (2018) modified the engine to enable the testing of high octane and oxygenated fuels, which was previously not possible. Although this CFR engine was uniquely modified, all modifications and standardisation checks were performed according to the ASTM D2699 and D2700 methods and included adherence to the compression pressure requirements.

3.2.2 Previous CFR modifications

The CFR engine at Stellenbsoch University was successfully re-commissioned by Bergenthuin (2018). The CFR engine underwent a complete engine inspection to conclude whether all tolerances for critical components, fell within the tolerances prescribed by the ASTM Manual for Rating Motor, Diesel and Aviation Fuels ASTM (1959). It was concluded that all measured components fell within the prescribed tolerances.

The CFR engine's cylinder wall and piston head were cleaned of any deposits. Deposits act as an insulation layer, reducing the overall heat loss from the air-fuel gas mixture to the cylinder walls and piston. This may result in an incorrect ON measurement, because with less heat transfer the test sample is more prone to knock and, therefore, lowers the measured ON. Over time, sufficient deposit formation can also increase the CR and therefore also lower the ON measurement causing measurement drift. This was observed by Foong *et al.* (2014), who performed RON and MON measurements using a CFR engine.

It has been well documented in literature that the standard CFR mixture heating and fuel flow rates are insufficient when measuring the MON values of oxygenated petrol blends. The heating deficiency is due to the higher latent heat of vaporisation (when compared to conventional fuels), which causes a strong cooling effect of the air-fuel mixture in the engine inlet manifold. The flow rate deficiency is related to the fuel's energy density. Ethanol, for example, is much less energy-dense than conventional fuels, therefore the achievable fuel flow rates are not sufficient when using the standard CFR fuel metering system.

Therefore, the recommendations described by Hunwartzen (1982) were successfully followed by Bergenthuin (2018) to modify the standard fuel metering and MON mixture heating systems to deal with these challenges. The fuel metering system was further modified in the current study and is outlined in Section 3.2.3. These modifications were successfully implemented in other studies such as those by Hunwartzen (1982), Johnson and Riley (1976), Anderson *et al.* (2010) and Foong *et al.* (2014), to solve the heating and fuel flow rate deficiencies.

The insufficient heating capacity of the air-fuel mixture was addressed by using auxiliary heaters to accurately control the mixture temperature according to the ASTM D2700 standard. In conjunction with the inlet air temperature heater used for RON measurements, two auxiliary heaters were used. Specifically, an internal heater is fitted inside the MON pipe and an external band heater is fitted around the outside of the MON pipe to control the MIXT. All heating elements are controlled by PID controllers and calibrated thermocouples. The MON pipe with auxiliary heaters is shown in Figure 3.3.

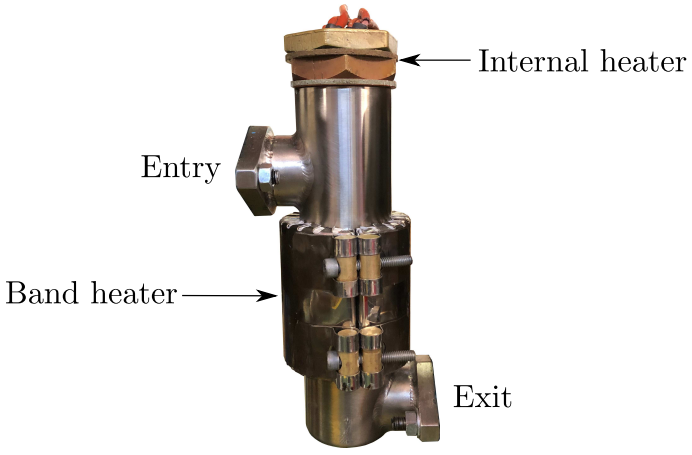

Figure 3.3: MON pipe fitted with auxiliary heaters used to control the air-fuel mixture temperature.

After modifications and the testing program performed by Bergenthuin (2018), it was concluded that Stellenbsoch University's CFR engine setup conformed to the ASTM standards. It was also concluded that results from preliminary round robin testing were comparable with those found in industry. Added to this: selected results from Foong *et al.* (2014) were replicated to

further serve as fit-for-use tests of Stellenbosch University's CFR engine setup (Bergenthuin, 2018).

With the knowledge that this CFR engine was comprehensively rebuilt and inspected by Swarts (2006) and Bergenthuin (2018), both according to ASTM specifications and both with credible and repeatable results, it was concluded that Stellenbosch University's CFR engine setup provided an excellent platform for investigating the underlying hypothesis of this study.

3.2.3 CFR modifications in the present study

Two new fuel metering devices were implemented in this study. The standard carburettor jets were replaced with adjustable orifice jets (needle jets) to accommodate the higher fuel flow rates required for testing of high octane and oxygenate fuels. The recommendations provided in the D2699, D2700 and German Institute for Standardisation (DIN) 51756-7 standards were followed.

Each needle jet is made up of a newly fabricated larger bore jet as well as a modified micrometer to act as the adjustable orifice, together with the jet. The spindle of the micrometer was machined to form a sharp needle, to fit inside the bore of the jet. The new jet and needle are shown in Figure 3.4.

(a) (b)

Figure 3.4: Adjustable orifice fuel metering device with (a) the new jet and the (b) modified micrometer needle.

The spark timing for RON remains constant at 13° BTDC, whereas for MON tests the spark timing is dependent on the CR (cylinder height). On newer CFR engines CR and spark timing adjustments are automatic. These adjustments are not automatic on Stellenbosch University's CFR engine and must be performed manually by the operator. For MON measurements, simultaneously adjusting CR and spark timing resulted in lengthy experiments. Therefore, as per the recommendations by (Bergenthuin, 2018), an electronic ignition system (EIS) using an engine control unit (ECU) was implemented to eliminate the extra time required for timing adjustments.

During the initial commissioning stages of the CFR engine, a new MON pipe needed to be fabricated, due to the mounting flange cracking during operation. A new MON pipe was fabricated as per the dimensions of the original pipe. The new MON pipe can be seen in Figure 3.3. It was decided that the validation of the new MON pipe's design was dependant on the ASTM fit-for-use tests (discussed later in Section 3.5). The CFR engine, fitted with the new MON pipe, met the ASTM fit-for-use specifications and was used throughout this project's testing program.

3.3 Gravimetric blending setup

Each liquid fuel test sample was blended using a volumetric gravimetric blending approach, as outlined in the ASTM standards. Mass measurements, based on the density of the individual components, were used. A digital balance scale, blending software and appropriate glassware including burettes, funnels and flasks, were used to blend test samples within a 0.2 %, by mass, tolerance limit (ASTM, 2019*a*,*b*). The digital scale was calibrated with calibration weights and was routinely checked.

In order to ensure no cross contamination of fuel components, only one burette was dedicated to each component and all flasks were thoroughly cleaned using distilled water and acetone after use. Each flask was left to dry in a dust free and locked blending room.

The blending software takes ambient temperature and fuel densities into account and provides real-time blending information for easy use by the operator. A detailed description of the blending equipment and software is provided Appendix A.

To ensure operator safety, all blends were performed within a ventilation hood, which extracts the working area of all harmful fumes. The operator also used appropriate personal protection equipment (PPE) at all times during fuel blending.

3.4 Selection of fuel components

In order to characterise the non-linear octane blending effects of important hydrocarbons and oxygenates, which make up the majority of the SI fuel recipe, it was necessary to select model fuel components, each representing the component class to which it belongs. For example, the aromatic toluene would represent all aromatics in the recipe, and so forth.

The component classes and components selected for this study are tabulated in Table 3.1, together with each component's Chemical Abstract Service (CAS) identification number. The CAS number is a numerical identifier assigned to every chemical substance described in open literature.

Table 3.1: Selected components studied in this project.

Class	Component	CAS #	Purity %
Olefin[a]	1-Hexene	592-41-6	96.61
Aromatic[a]	Toluene	108-88-3	99.01
Alcohol[b]	Ethanol	64-17-5	99.91
Ether[b]	TAME	994-05-8	97.70
Isoparaffin[a]	Isooctane	540-84-1	99.47
n-Paraffin[a]	n-Heptane	142-82-5	98.87
Cycloparaffin[a]	Cyclohexane	110-82-7	98.80
NMOB[c]	2,4-Xylidine	95-68-1	N/A

[a] Hydrocarbon
[b] Oxygenate
[c] Non-metallic octane booster

Each component in Table 3.1 was chosen based on the component's ability to accurately represent the class to which it belongs as well as its previous usage in distinguished literature on octane blending.

Natural first choices for the paraffinic (alkane) and aromatic components are the PRFs (n-heptane and isooctane) and toluene, respectively.

Due to the studies by Swarts (2006) and Viljoen (2009), 1-hexene was selected to represent the olefin class. Also, Foong *et al.* (2014) reports 1-hexene as a good choice for representing the olefin class for petrol surrogate formation. 1-Hexene has also been a popular choice to represent olefins in various fuel blending and chemical kinetic models studies (Perez and Boehman, 2012).

For the alcohol component, ethanol was chosen, based on its significant interest and usage in recent years. Ethanol is also preferred over other alcohols and oxygenates, such as MTBE for example, due to its preferred environmental effects (Kenny, 2013).

TAME was selected to represent the ether class. This choice was based on the fact that high purity TAME is produced by Sasol and was readily available. Little octane blending data is available for TAME, therefore, this study provided a platform to investigate this ether's octane blending properties

from a refineries point of view. Added to this, Mirabella *et al.* (2016) states TAME to be one of the more popular choices amongst ether based octane enhancers, used by refineries.

Cyclo-paraffins are important constituents of the petrol recipe, therefore, in addition to the above, cyclohexane was chosen to represent the cyclo-paraffins class. This selection was also based on the component's availability and its role in representing the cyclo-paraffin family.

Included in the project scope, was the testing of a non-metallic octane booster (NMOB): 2,4-Xylidine. This NMOB was added in small percentages by volume to all of the components listed in Table 3.1 as well as locally purchased commercial un-leaded petrol (ULP) from two different sources.

An important aspect of this research was to characterize the octane blending effects of these selected components, on a fundamental level. This involved the procurement of high purity fuel components according to the ASTM purity specifications. Each component was sent to a chemical laboratory for gas chromatography-mass spectrometry (GC-MS) tests to obtain the purity percentages of each component. It must be mentioned here that a large part of the project time line was taken up by the iterative process of procuring high purity components, which are indeed pure components and not isomers with varying octane qualities. These purity values are also listed in Table 3.1.

3.5 Experimental octane testing methods

In order to meet the project's aims and objectives, the experimental testing was split up into various phases. The various phases included engine standardisation tests, the generation of a characteristic curve (CC) for the CFR engine, the pure component testing, followed by the binary testing phase. These phases are outlined in this section.

3.5.1 Phase 1: Characteristic curve (CC) generation

Phase 1 was aimed at the generation of a CC for the CR method for measuring RON and MON. The CC relates a measured ON to a corresponding CR and is specific to a particular CFR engine. The CR is directly related to the dial micrometer reading, indicating the head height. Previously Bergenthuin (2018) established this relationship by following the liquid fill method, prescribed by the ASTM standards (ASTM, 2019*a*,*b*).

To generate the RON and MON CCs, standard KI was obtained for various blended PRFs at different CRs. Two CCs were generated and used for the

relevant RON and MON experiments. A reference value for each of the CCs is listed in the ASTM standards and was used for the CC generation (ASTM, 2019*a*,*b*). Using isooctane and under standard operating conditions, standard KI was obtained at a dial gauge reading of 0.454 inch for RON and 0.392 for MON, correlating to a CR of 7.77 for RON and 8.46 for MON. This step was verified at the beginning, during commencement and after of each experimental testing period.

By definition, using PRFs, the maximum ON that can be obtained is 100. In the past Tertaethyl lead (TEL) was the 'golden standard' for anti-knock fuel additives and was used in small quantities to blend ONs higher than 100. However, since its use is no longer permitted, it has become obsolete. Besides the fact that TEL is a very toxic component, it is also not easily obtainable. Therefore, to extend the measurable range, toluene was used to increase the RON CC to 120 and the MON CC to 107. This approach was also adopted by Kalghatgi *et al.* (2014).

The CR method was adopted in this study due to the time efficiency. The CR method was successfully adopted by Kalghatgi *et al.* (2014) Anderson *et al.* (2012), Foong *et al.* (2014), Yuan (2018), da Silva Jr *et al.* (2019) and Swarts (2006) and Bergenthuin (2018) using the same CFR engine as used in this study.

This study involved an extensive testing program, allowing a large initial characterisation of the unknown octane blending interaction effects found between binary combinations of all of the components listed in Table 3.1. The CR method was also shown to provide repeatable and accurate results, in accordance with the ASTM D2699 and D2700 standards. However, the RON and MONs of the pure components were also bracketed using PRFs and the bracketing method. Various other randomly chosen blends throughout the experimental phase were also bracketed using PRFs, to regularly verify the CR method results.

3.5.2 Phase 2: Fit-for-use engine tests

According to the ASTM standards, each fuel sample ON measurement shall be performed using a qualified CFR engine. A CFR engine is qualified by performing fit-for-use tests known as toluene standardised fuel (TSF) tests. A CFR engine must be qualified atleast once every 12 hours or after an engine shut down period of at least two hours. All TSF blends shall be unchilled and rated without carburettor cooling.

TSF fuels are volumetric blends of toluene, n-heptane and isooctane, calibrated by the National Exchange Group Laboratories (ASTM, 1959). TSF

fuels are highly volatile blends and are sensitive to component purities and blending accuracies. More importantly, ON measurements are greatly affected by any variations in engine irregularities, measurement equipment, operator methods and the condition of the combustion chamber.

Blending data for each TSF is listed in the D2699 and D2700 ASTM standards. Each TSF blend has an octane number tolerance band, that a CFR engine must adhere to when measuring each TSF. If a measured TSF falls outside of the specified tolerance, the IAT and MIXT can be adjusted by the operator, to bring the measured TSF within tolerance. For RON the IAT is tuned and for MON the IAT remains constant, while the MIXT is tuned. Table 3.2 lists the temperature ranges for TSF tuning for RON and MON.

Table 3.2: Adjustable ranges for IAT and MIXT TSF tuning.

Parameter	RON	MON
IAT*	52 °C ± 22 °C	38 °C ± 2.8 °C
MIXT*	Not controlled	141 °C ≤ MIXT ≤ 163 °C

* All temperatures within ± 1 °C, unless specified otherwise (ASTM, 2019*a*,*b*).

In order to initially standardise Stellenbsoch University's CFR engine, before any component testing, all RON and MON TSF tests were performed to make sure that the results fell within the ASTM TSF specified tolerances. The CR method and the bracketing method were used and confirm that the operator's procedure was fit-for-use as well. TSF tests were also performed regularly during each experimental period, dependent on the required octane measuring range.

It was also decided by the author to use isooctane as a further fit-for-use criteria. Because the RON and MON values of isooctane are ASTM defined, isooctane was tested before, during and after each experimental testing phase to essentially 'bracket' every testing period for any engine measurement drift, irregularities and more importantly operator error.

3.5.3 Phase 3: Pure component testing

Phase 3 included the RON and MON measurements of each of the pure components. As mentioned before all RON and MON tests of the pure components were further bracketed using PRFs for improved accuracy and certainty. This was an important step in the experimental phase because these results were used for the empirical estimations as well as comparative purposes to literature.

As per the ASTM standards, the RON and MON values of the two PRFs are defined by definition. For n-heptane, both RON and MON are defined as zero. For isooctane, both RON and MON are defined as 100. The sensitivity for both PRFs is therefore also defined as zero.

The RON and MON of pure toluene is critical because it forms part of the TSF fuels used for qualifying the CFR engine during each operating period. Foong *et al.* (2014) reported difficulty in measuring the high RON of neat toluene, which approaches the upper limit of the CFR engine's measurable range. However, after modifications by Bergenthuin (2018), measurements at these high RON values is now possible.

As mentioned before, toluene was used to extend the measurable range above a RON of 100. Therefore, the RON value of toluene was pre-defined using RON values found in literature. Foong *et al.* (2014), the API dataset and Heywood (1988) report the same RON value of 120 for toluene.

The RON and MON values of neat TAME vary in literature and are usually reported as calculated blended octane numbers (BON), and not actual measured ONs of neat TAME. This further enforces the choice of TAME to represent the ethers class, since valuable RON and MON octane data was obtained for TAME in this study, using the ASTM prescribed methods. Mirabella *et al.* (2016) performed a thorough literature study on octane data pertaining to ethers commonly used by the refining industry. Mirabella *et al.* (2016) also includes the data of TAME produced by Sasol.

There are numerous octane data sets for neat and blended ethanol, however, it is believed that the measurements obtained by Hunwartzen (1982) and Foong *et al.* (2014) are the most reliable, since they comply with the ASTM and DIN standards.

Measuring the RON and MON of the NMOB was not possible because the NMOBs ON exceeds the measurable range of the CFR engine.

3.5.4 Phase 4: Binary component blending

Only after Phases 1-3 were completed, Phase 4 could commence.

Fully charactering the non-linear octane blending behaviours of all the selected components was not within the scope of this project. Therefore, it was decided to begin with 50/50 binary blending behaviours, that is, a blend composition of equal volume percentages of two components. Initially testing all combinations of the selected components at these 50/50 blends provided a platform for comparisons between actual measured results and the empirically

calculated results.

3.5.5 Phase 5: Further characterising the non-linearities

The results from Phase 4 prompted the investigation of measuring the blend ratios on either side of the 50/50 midpoint. Initially blend ratios of 25/75 (blend of 25 % of one component and 75 % of another) and 75/25 were chosen and later adapted to 15/85 and 85/15, after the binary 1-hexene blends were completed.

This choice was based on the following:

1. Additions to the petrol recipe usually include small percentages of components, therefore the new ratios align better with refinery economics.
2. Chebyshev's inequality states that at least 93.75 % of the data must be within two standard deviations from the mean, therefore supporting the ratio change towards the extremes of the composition.

Extension of the blend matrix to include all of the above blend ratios was a large undertaking and took up the majority of the project's time-line. However, as presented in Chapter 4, the results isolate many synergistic and antagonistic behaviours. These results also align well with establishing conclusions for the project's hypothesis.

3.5.6 Non-metallic octane booster testing phase

Part of the project scope was to test the octane additive properties of a NMOB, 2,4-Xylidine. The NMOB was added in 1, 2 and 3 % ratios to each of the selected components. The testing of this NMOB revealed its ability to boost the octane of the component, into which it was blended.

Chapter 4

Experimental results

This chapter presents the project results obtained from the engine experiments outlined in Chapter 3.

4.1 Characteristic curve (CC) generation for RON and MON

The generation of a CC for both RON and MON methods was accomplished by blending and measuring various PRF blends. Figure 4.1 shows the CCs produced for Stellenbosch University's CFR engine, for this project as well as in previous projects.

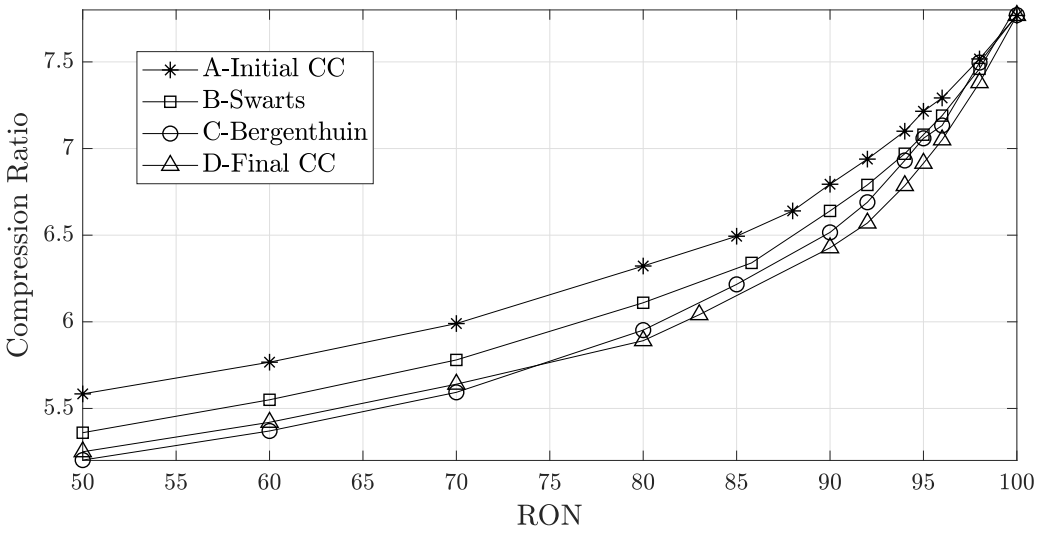

Figure 4.1: RON Characteristic Curve (CC).

Both Swarts (2006) and Bergenthuin (2018) adopted the CR method using a CC. Figure 4.1 shows that the CC by Bergenthuin (2018) is lower than that of Swarts (2006), verifying the improved compression of the engine after upgrades and modifications. One can also see that all the curves converge at a RON of 100. This is because this point was used for the curve calibration (starting point) as well as the KI meter calibrations, according to the ASTM standards.

It was assumed that the CC generated for this project, would match the CC by Bergenthuin (2018) as no major engine modifications or disassembly was performed in this project and this project was a direct continuation from that of Bergenthuin (2018). However, the initial RON CC ('Initial CC' in Figure 4.1) is positioned higher than that of Bergenthuin (2018). It was found that the procured n-heptane component was not pure n-heptane, but a contaminated mixture of isomers. New n-Heptane was sourced, tested for purity and then used in the generation of the final RON CC for this project ('Final CC' in Figure 4.1).

Upon observation, the final CC closely matches that of Bergenthuin (2018), as initially expected. It was concluded that any differences in the two curves were results from the two different engine operators. A similar approach was used to generate the CC for the MON configuration. The final CCs for RON and MON for the present study are shown in Figure 4.2.

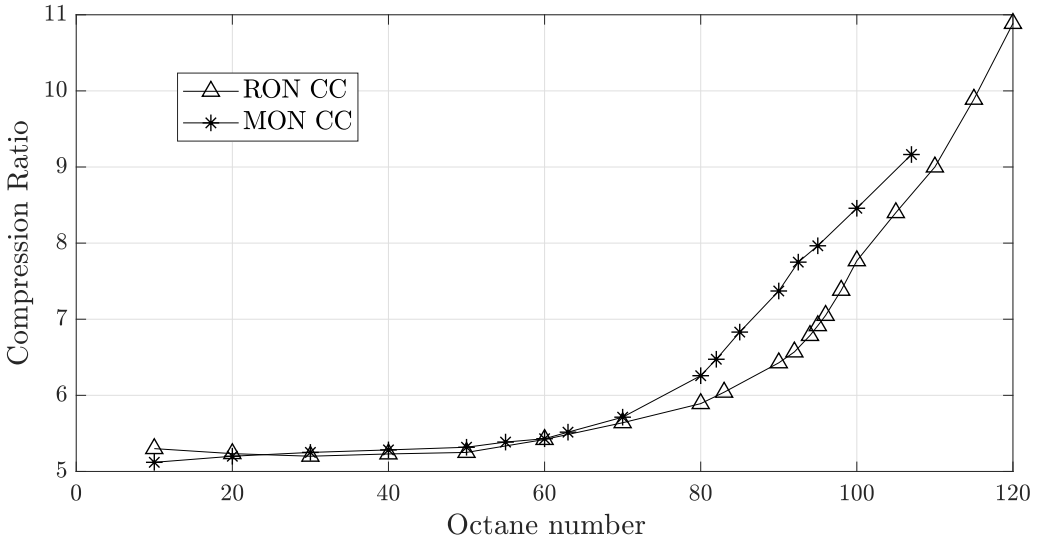

Figure 4.2: Final RON and MON characteristic curves (CC) for Stellenbosch University's CFR engine.

Generation of the CCs proved challenging, due to various factors. Firstly, generating a CC that produces accurate TSF results, for the entire TSF fit-for-use qualifying range is a large iterative exercise. Secondly, there were other engine specific test features, that played a role in maintaining the ASTM operating conditions. Examples include spark energy, maintaining constant spark timing and noise disturbances in speed control. A discussion of these variables is provided in Appendix B.

4.2 CFR qualification

Phase 2 involved qualifying the CFR engine according to the ASTM standards, by performing TSF tests. All TSFs were blended and measured using two methods: the CR method and the bracketing method outlined in Section 3.5. This, in turn, validated the CCs by bracketing the CCs interpolated results with PRFs. The measured RON TSF results and the respective TSF tolerance bands, specified in the ASTM standards, are shown in Figure 4.3.

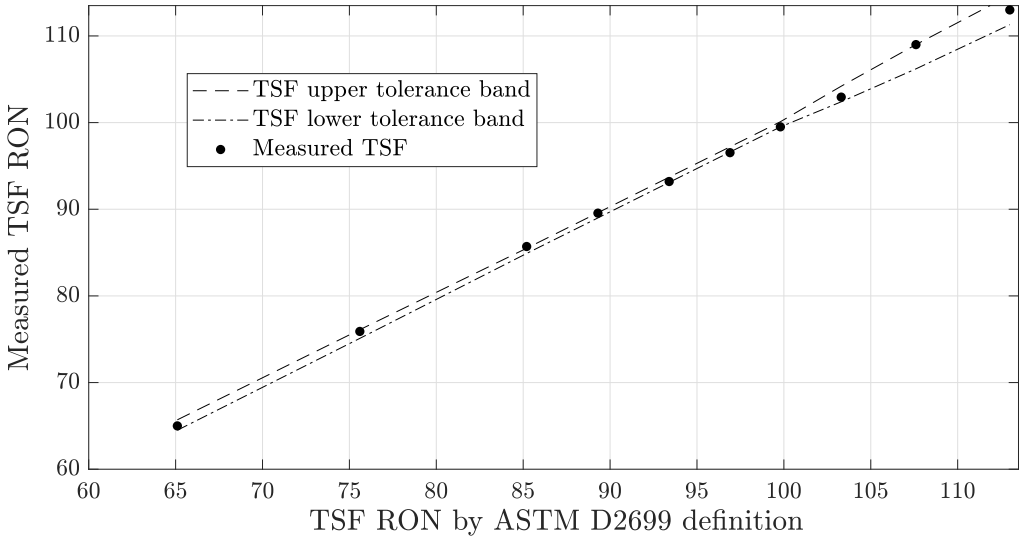

Figure 4.3: Measured TSF results for RON.

The measured MON TSF results are graphed in a similar manner in Figure 4.4.

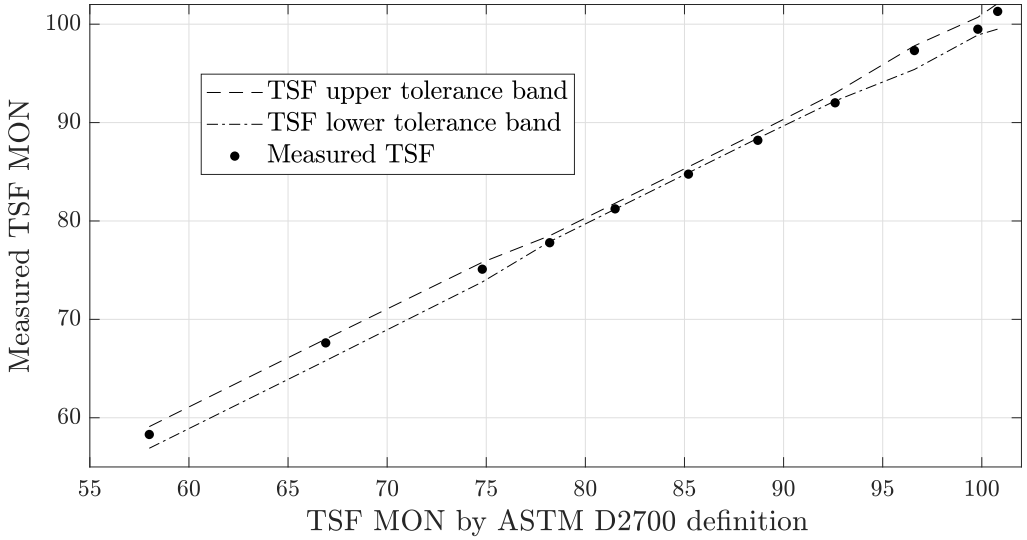

Figure 4.4: Measured TSF results for MON.

As shown in Figures 4.3 & 4.4, the measured TSFs fall within the ASTM specified tolerance bands, concluding that Stellenbosch University's CFR engine setup and CCs are fit-for-use and qualified according to the ASTM standards. For RON an IAT of 52 °C was set. For MON the IAT was set to the standard IAT of 38 °C ± 2.8 °C, and a MIXT of 142 °C was selected for MON.

It must be noted here that this phase involved many additional hours of testing to initially qualify the CFR engine at these IAT and MIXT temperatures, for the entire measurable range. This is because there are many other variables (excluding IAT and MIXT adjustments), which influence the highly volatile TSF fuel measurements. These include, maintaining constant spark timing and noise disturbances in speed control of the dynomometer.

An important note: in addition to this initial CFR qualification of the entire measurable ON range, was the qualification of every experimental testing period. This was accomplished by blending and testing TSFs fit for the possible measurable ranges of the fuel samples to be tested. This is prescribed in the ASTM standards and the relevant TSFs and ON ranges they cover can be found in the ASTM standards.

4.3 Pure component testing

As per the ASTM standards, the RON and MON values of the two PRFs are defined by definition. For isooctane, both RON and MON are defined as 100. For n-heptane, both RON and MON are defined as zero. The sensitivity for both PRFs are therefore also defined as zero.

The RON and MON measurement of neat n-heptane was not within the measurable range of Stellenbosch University's CFR engine. The lowest and highest ON measurement is also physically dependent on the possible CR adjustment range to maintain combustion, which was unknown at project commencement. Therefore, PRFs were blended and tested in an iterative process to obtain the lowest and highest CRs possible using this CFR engine. The lowest and highest measurable RON values were 10 and 120, respectively.

The RON and MON of each of the neat components (excluding the NMOB) listed in Table 3.1 was measured. An initial ON was obtained using the CR method and CCs, after which, the bracketing method was used to bracket the test samples, for improved accuracy and certainty. Table 4.1 lists the measured RON and MON values of the selected components for this project as well as RON and MON values found in literature. Both the RON and MON of isooctane and n-heptane are by definition and are excluded from Table 4.1.

Table 4.1: Measured and reported RON and MON of neat components.

Component	RON meas.	RON lit.	API	MON meas.	MON lit.	API
1-Hexene	75.70	73.60[1]	76.40	63.30	64.50[1]	63.40
Toluene	120	120[2]	120.10	107	107[2]	103
Ethanol	108	108.25[2]		90.20	90.70[2]	
TAME	110.40	110[3]		96.30	99.10[3]	
Cyclohexane	83.70	83[4]	83	79.90	77.20	77.20[4]

Literature sources:
[1] Badra *et al.* (2017)
[2] Foong *et al.* (2014)
[3] Mirabella *et al.* (2016)
[4] Guibet (1991)

As mentioned in Section 3.5.3, measuring the RON and MON of the neat NMOB exceeds the measurable range of the CFR.

4.4 Binary blends

4.4.1 Overview

The binary blending interaction effects between all of the selected components at various blend ratios were investigated. Please refer to Section 3.5.4 for more information on the blending ratio selections and experimental methodologies.

Also included in this section, are the octane estimations using two well known empirical models: the Stewart (Stewart, 1959) and Ethyl (Healy *et al.*, 1959) models. This allowed valuable insight into these model's abilities to predict the actual measured octane blending non-linearities, present in the blend.

Before the graphed results are presented, it is first necessary to explain how to interpret the information. Figure 4.5 is an example graph of a binary combination of 1-hexene blended into cyclohexane.

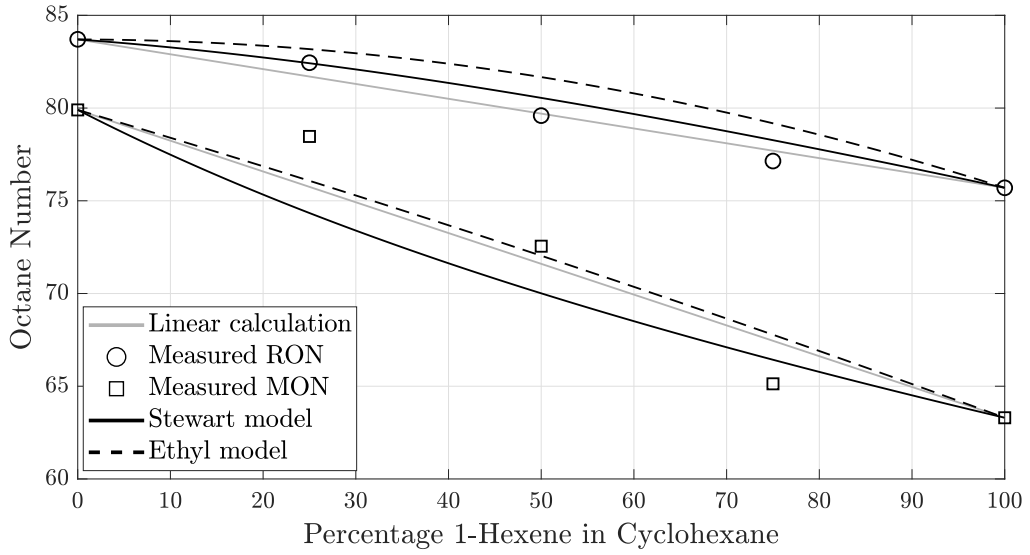

Figure 4.5: RON and MON binary blend results for of 1-hexene blended into cyclohexane.

Volume percentage composition is given on the horizontal axis and the measured ON on the vertical axis. Each graph has both RON and MON data, with the RON data always positioned above the MON data. According to the legend: the measured data is plotted as either circles for RON or squares for

MON, the linear blend calculation are plotted as straight lines and the Stewart and Ethyl models are as per the legend. The data points at the extremes of the horizontal axis are the measured ONs of the pure components in the blend. For example, in Figure 4.5, zero on the horizontal axis is the RON/MON of pure cyclohexane and 100 is the RON/MON of pure 1-hexene.

In terms of the Stewart and Ethyl model data, it is important to note the following: the Stewart model becomes a linear calculation when no olefin content is present in the blend, and similarly the Ethyl model shows very small non-linearities (due to the sensitivity term) when there is no olefin and aromatic content.

The visualisation of the OS is a powerful aspect of each graph. This was discussed in Section 2.2.3. For example, for the MON measured results in Figure 4.5, one can see that the sensitivity increases, with increasing 1-hexene (olefin) content. Therefore, OS can be seen as a function of blend ratio by observing how the delta between the RON and MON lines change with blend ratio.

By comparing Figure 4.5 to Figure 2.5, one can already draw conclusions in line with the project's hypothesis. For example, with increasing addition of 1-hexene, the OS increases and therefore shows which blend ratio, in this specific binary blend, is more suitable to modern SI IC engines. A summary table for all the binary blend results is included at the end of this chapter. Please refer to Appendix C for the raw experimental data.

4.4.2 Binary blend results

The following figures present the binary blend measured results, together with model predictions using the Stewart and Ethyl models. Each figure contains six graphs: each selected component blended into every other component in increasing blend ratios (please refer to each graph's horizontal axis for blend reference). Each figure's legend is included at the top of the figure. Commentary on these figures is provided after all the graphed results in Section 4.5.

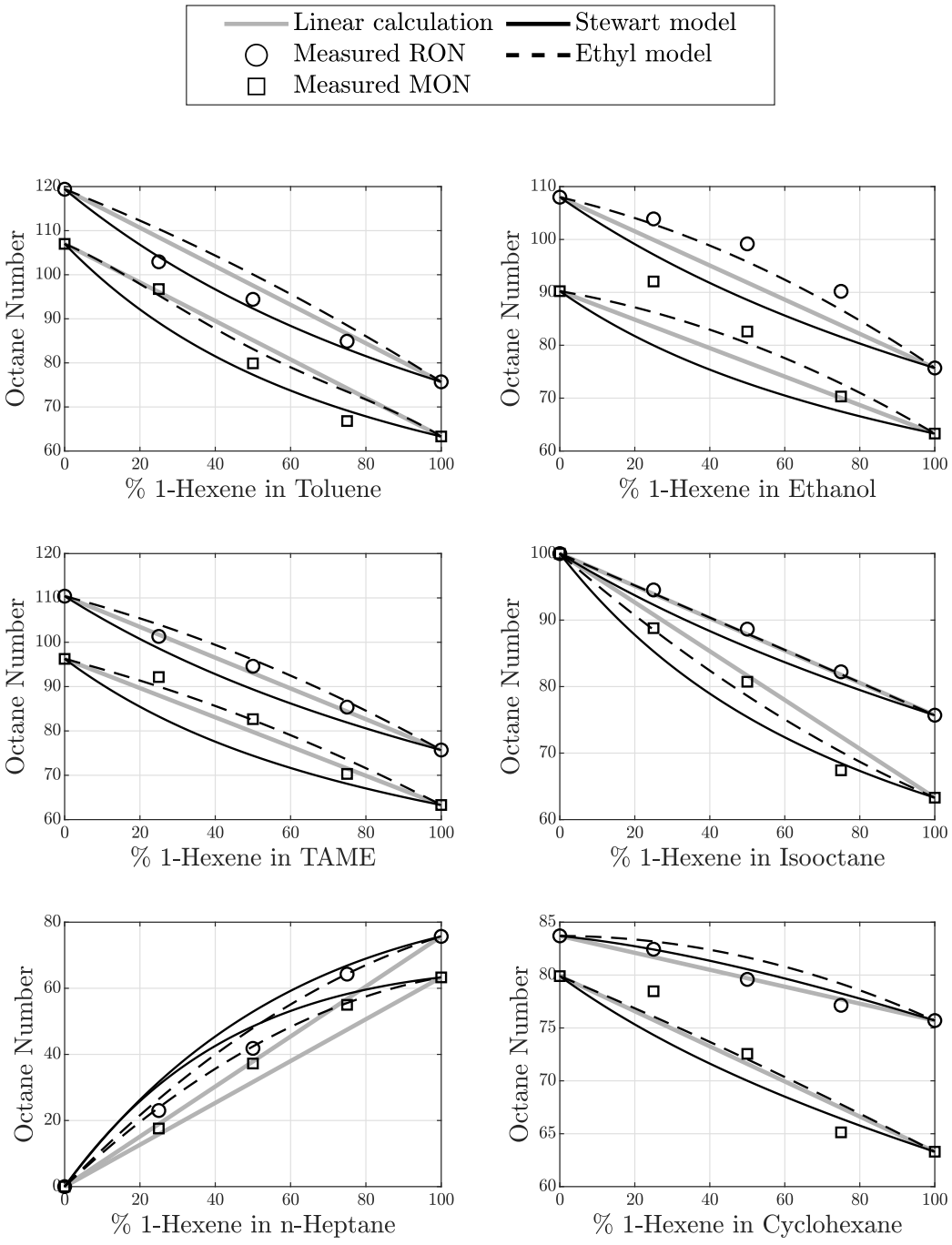

Figure 4.6: Binary 1-hexene blends.

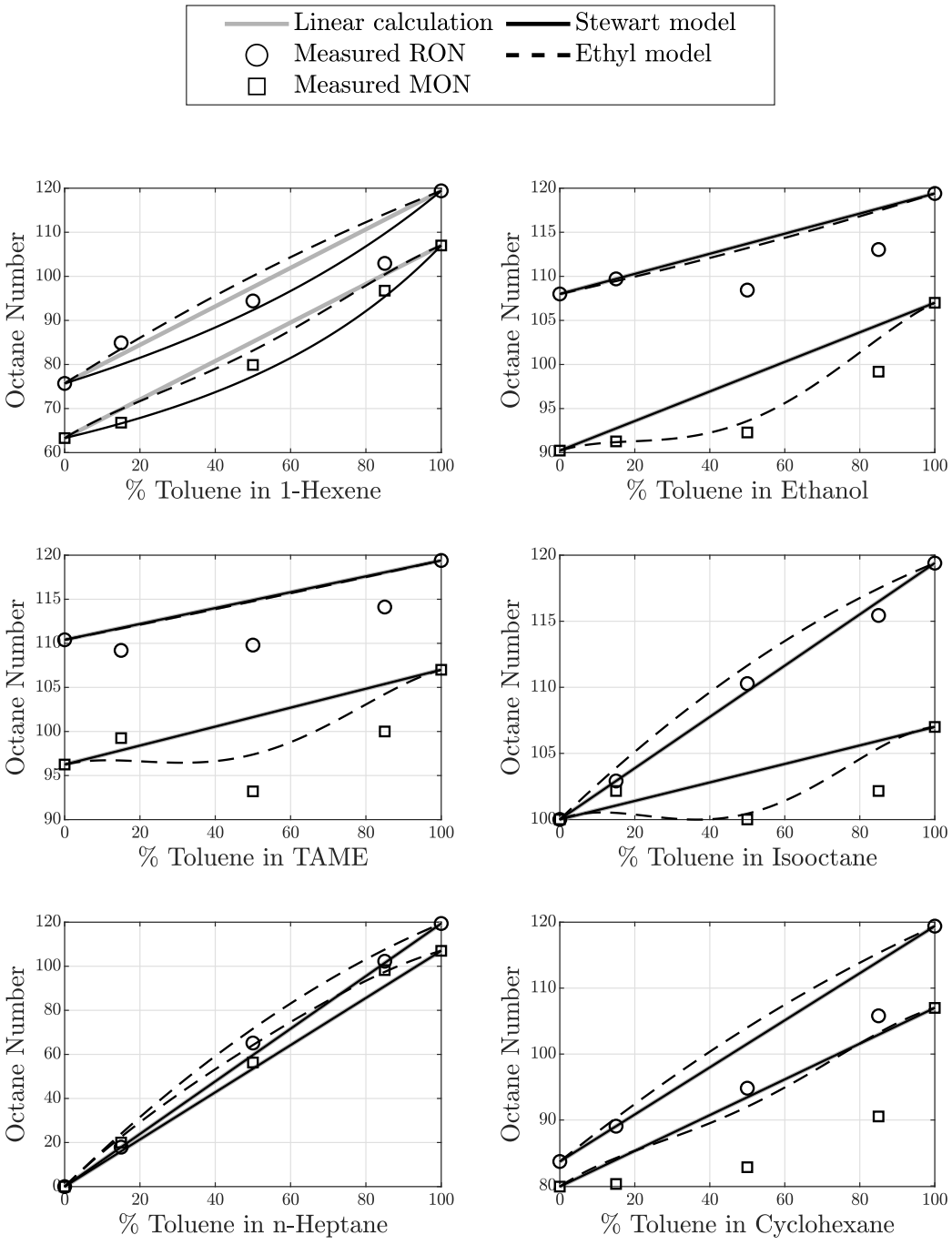

Figure 4.7: Binary toluene blends.

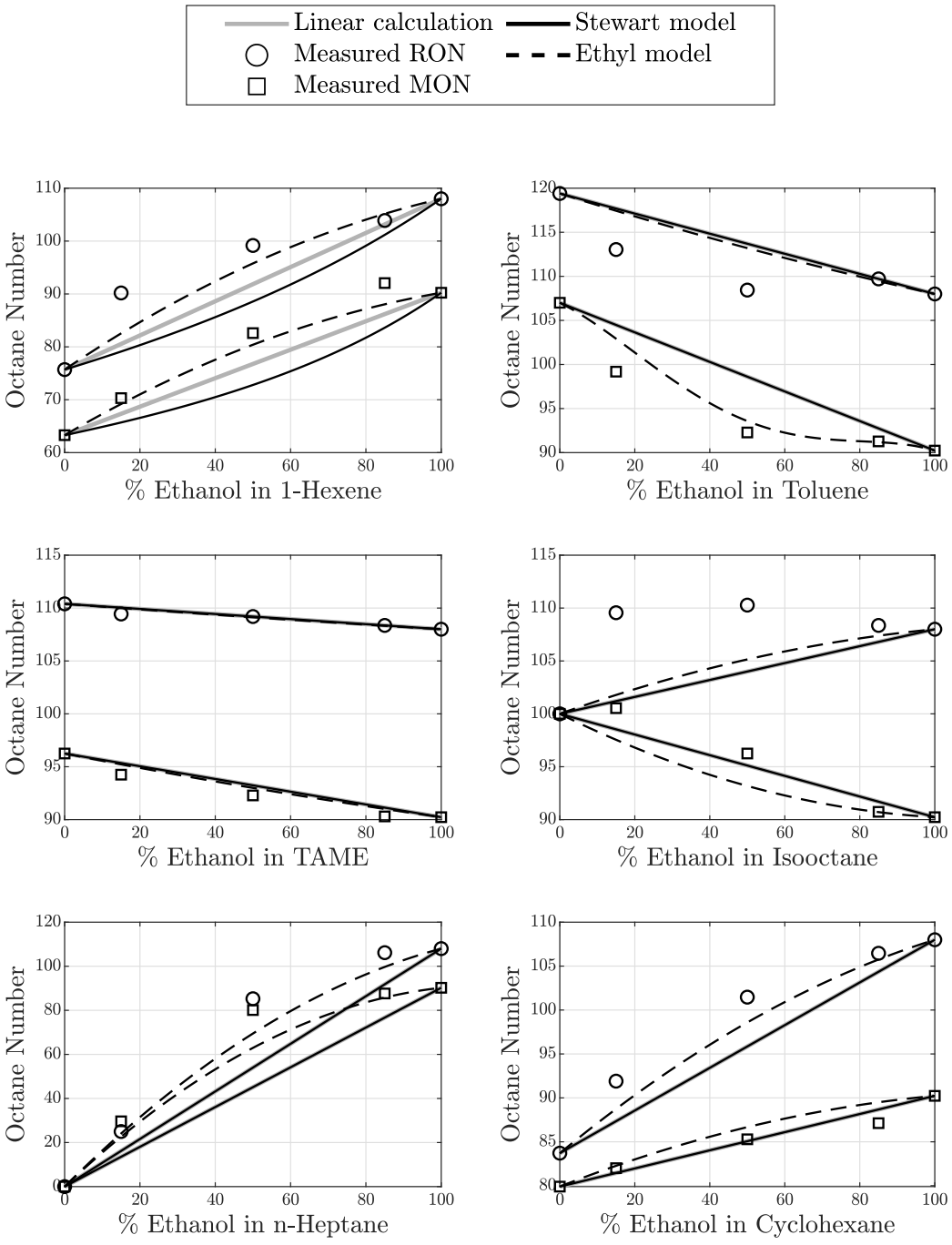

Figure 4.8: Binary ethanol blends.

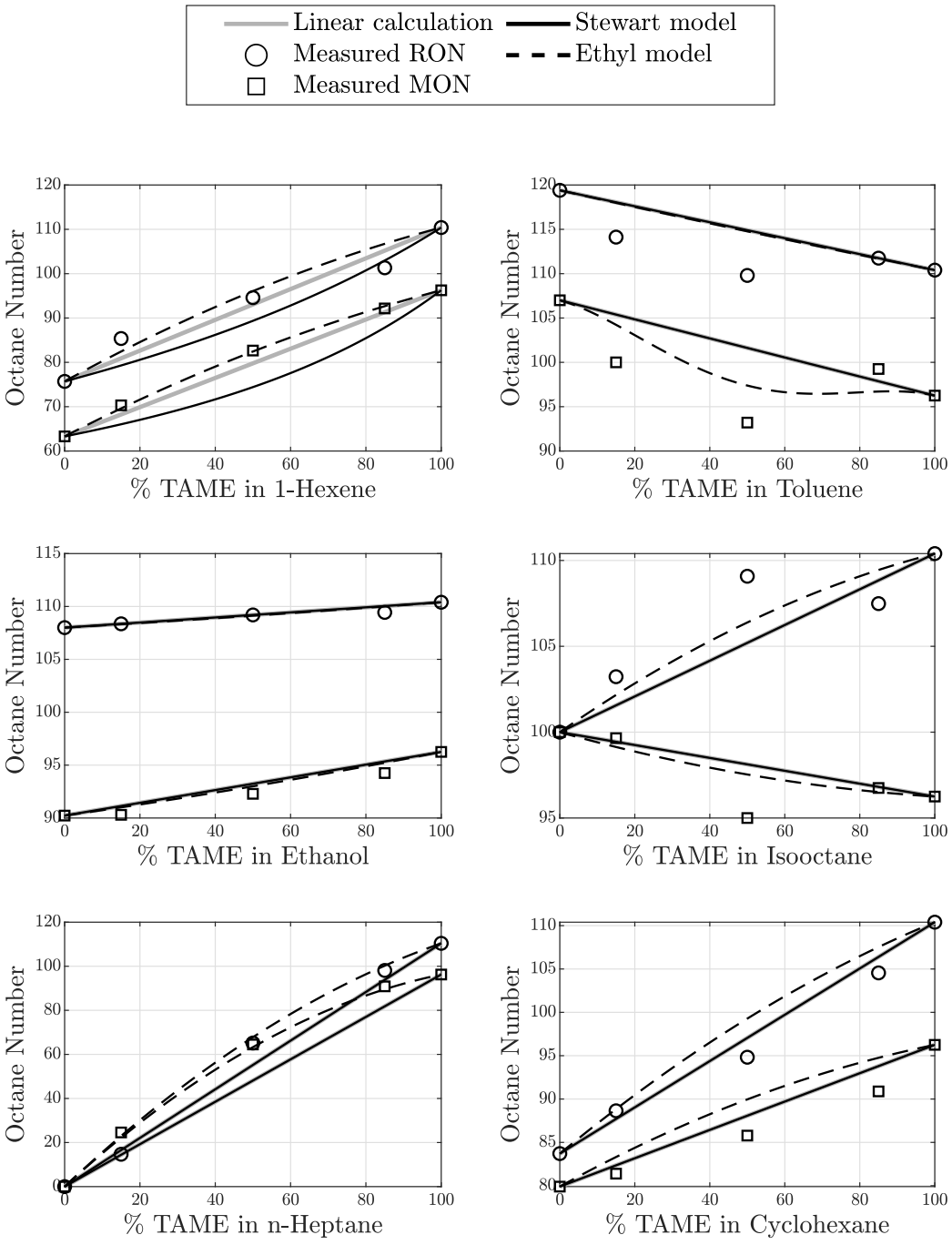

Figure 4.9: Binary TAME blends.

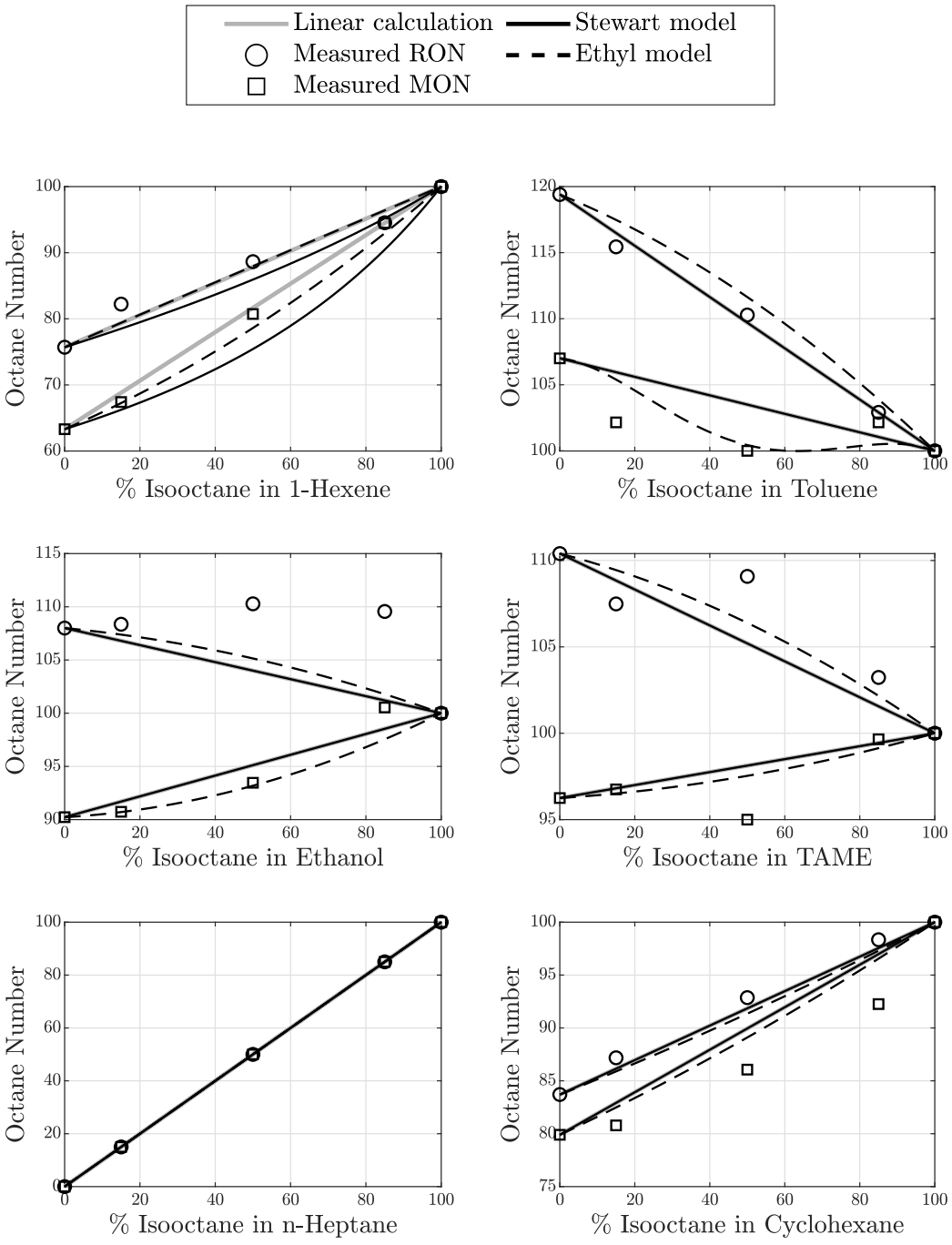

Figure 4.10: Binary isooctane blends.

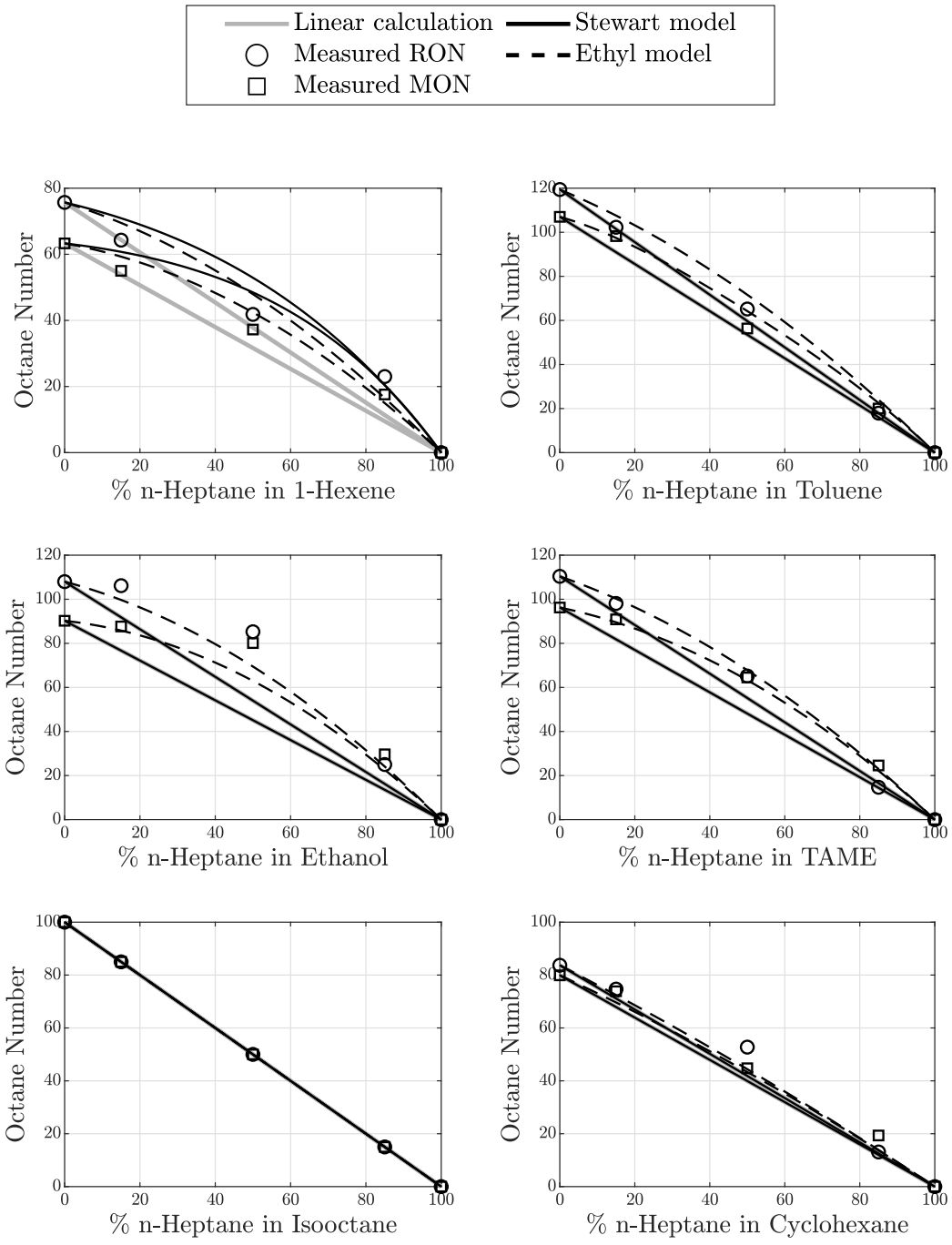

Figure 4.11: Binary n-heptane blends.

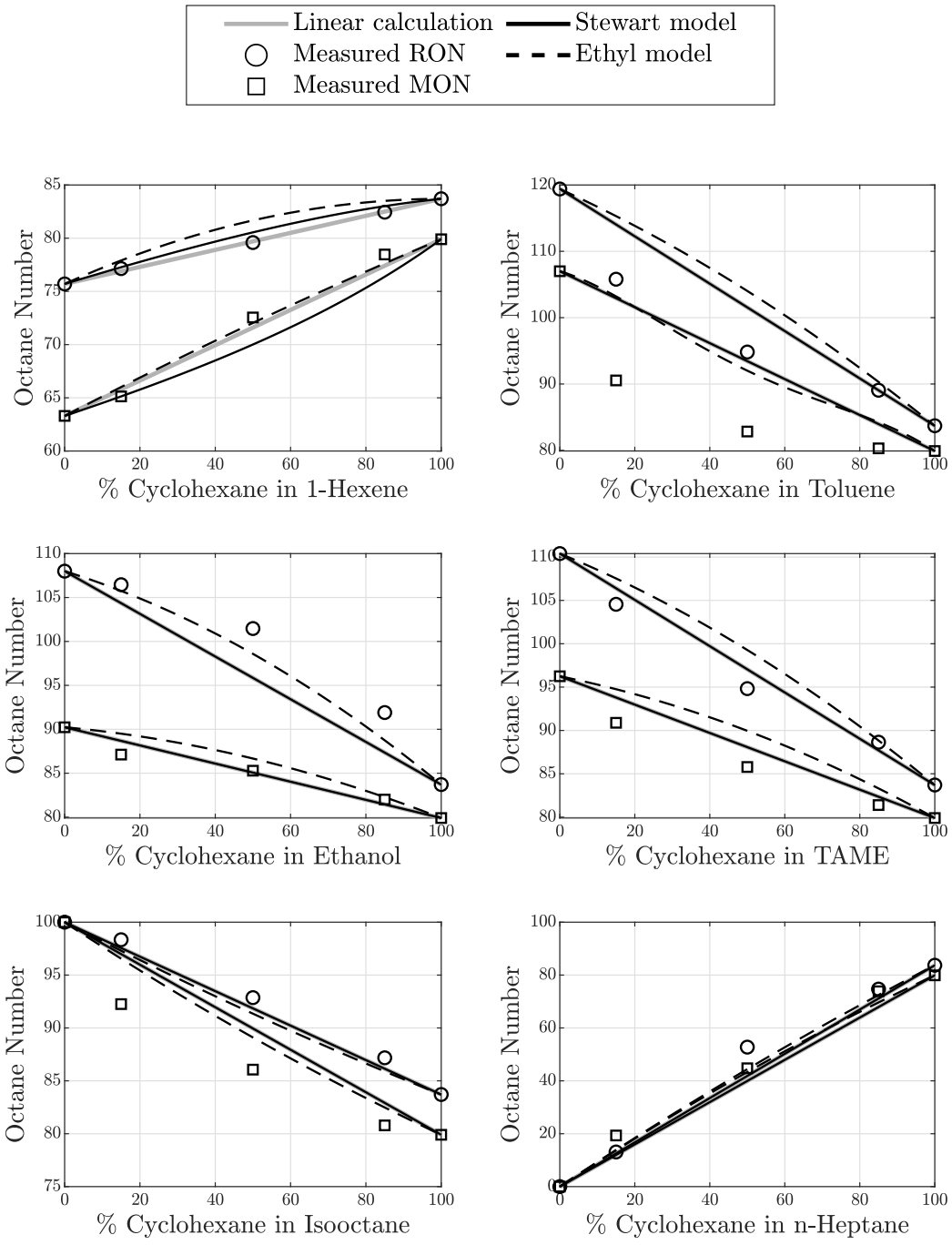

Figure 4.12: Binary cyclohexane blends.

4.5 Binary results summary

Various octane blending behaviours were observed: either linear (L), synergistic (S), antagonistic (A) or combinations of the three. Each binary combination has been summarised by assigning either a L, S or A to each of the blend ratios. Table 4.2 summarises the RON results and Table 4.3 summarises the MON results. Please refer to Section 6.6 for a more in depth discussion on these results.

Using the same example in Figure 4.5, the entry in Table 4.2 for the 1-hexene/cyclohexane (1-hexene blended into cyclohexane) combination is 'SLA' which designates a synergism at the 15/85 ratio, linear blending at the 50/50 point and antagonism at the 85/15 blend ratio.

Table 4.2: Summary of RON binary blending interactions.

Component	hex	tol	eth	tame	iso	n-hep	cyc
1-hexene		AAA	SSS	LSS	SSS	SSS	SLA
toluene			LAA	AAA	LSA	LSL	LAA
ethanol				ALL	SSS	SSS	SSS
TAME					SSA	ASS	SAA
isooctane						LLL	SSS
n-heptane							SSL
cyclohexane							

[S] Synergistic
[A] Antagonistic
[L] Linear

Table 4.3: Summary of MON binary blending interactions.

Component	hex	tol	eth	tame	iso	n-hep	cyc
1-hexene		SAA	SSL	SSA	AAA	ALA	SLA
toluene			AAA	SAA	SAA	LSS	AAA
ethanol				AAA	SSL	SSS	SLA
TAME					SAA	SSS	AAA
isooctane						LLL	AAA
n-heptane							SSS
cyclohexane							

[S] Synergistic
[A] Antagonistic
[L] Linear

The predictions using the Stewart and Ethyl models were also investigated. To distinguish which model better predicted the non-linearities in the measured data, the standard errors (SE) were calculated. The SE was calculated using Equation 4.1.

$$Standard\ error = \sqrt{\frac{\sum(x_{measured} - x_{predicted})^2}{N}} \tag{4.1}$$

Where, N is the number of data points.

Table 4.4 lists the SEs between the two models' predictions and the measured data as well as the SE between the LBV calculation and the measured data.

Table 4.4: Standard errors (SE) of each prediction model.

SE	LBV	Stewart model	Ethyl model
RON	15.34	14.83	5.49
MON	9.42	11.74	4.97

Table 4.4, concludes that the Ethyl model better predicts the measured data, when compared to the Stewart model and also enforces the general trend that a LBV calculation is no longer accepted in industry.

Although the binary blends studied in this project are far removed from typical refinery blends, and while the Stewart and Ethyl models have been shown to work well on typical refinery blends, their weaknesses were highlighted in this project, using fundamental components. This aligns well with one of the specific aims of this research.

4.6 Non-metallic octane booster (NMOB) testing

The NMOB 2,4-Xylidine was added in 1, 2 and 3 % by volume ratios, to each of the selected components and unleaded petrol (ULP) 95. ULP 95 was sourced from two different local petrol suppliers and similar results were obtained for both.

The RON results are shown in Figure 4.13. The results for n-heptane are plotted separately, for scaling purposes, in Figure 4.14.

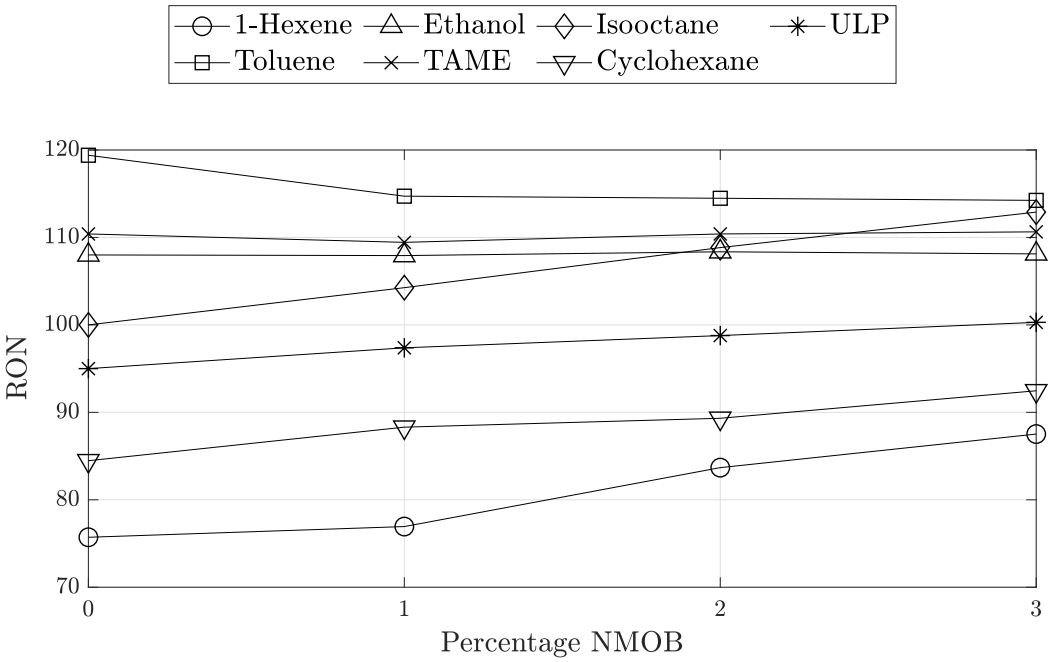

Figure 4.13: RON binary blend results for NMOB added to components listed in legend in 1, 2 and 3 % by volume ratios.

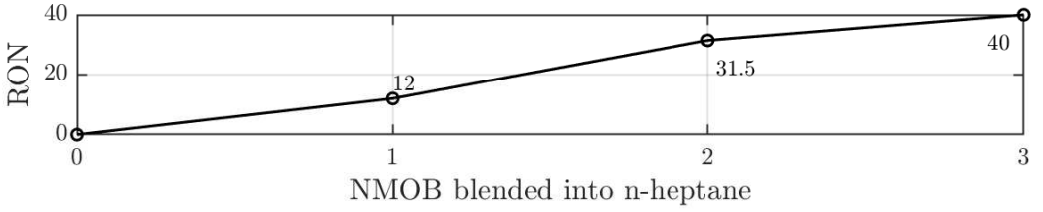

Figure 4.14: RON results for NMOB blended into n-heptane in 1, 2 and 3 % ratios.

The MON results are shown in Figure 4.15 and Figure 4.16, graphed in a similar manner to the RON results.

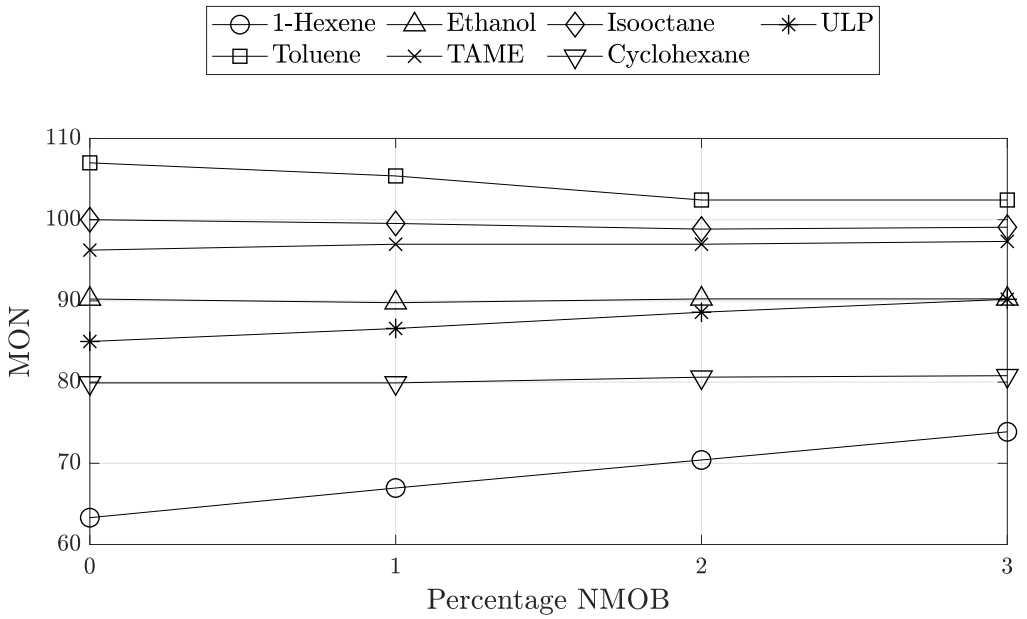

Figure 4.15: MON binary blend results for NMOB added to components listed in legend in 1, 2 and 3 % by volume ratios.

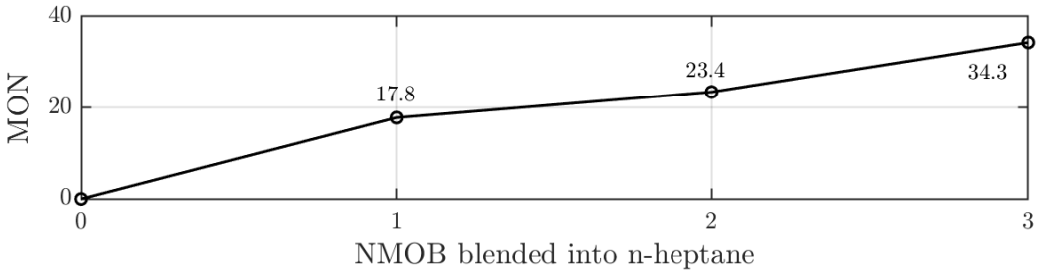

Figure 4.16: MON results for NMOB blended into n-heptane in 1, 2 and 3 % ratios.

Please refer to Section 6.7.1 for an in depth discussion of these results.

Chapter 5

Development of an improved octane prediction model

5.1 Overview

The Stewart and Ethyl models' prediction capabilities were investigated in Section 4.4.2. It was found that the Ethyl model better predicted the measured data when compared to the Stewart model. The Ethyl model includes additional non-linear terms, over and above the Stewart model, therefore, it was decided to optimise and improve the Ethyl model's predictive capabilities.

It is understood that the optimisation of a generalised prediction model, using a small data set, will generally improve the model's predictive capabilities, however, may worsen the predictions of larger and more complex refinery-specific blends. Nonetheless, by using this data set, potential mathematical deficiencies in the Ethyl model can be identified and the improved model can be optimised to larger refinery-specific blends, since the deficiencies of the model have been rectified.

The objectives of this chapter was to therefore:

1. Optimise the standard Ethyl coefficients using the measured data to enable comparisons to a new mathematically improved Ethyl model.
2. Investigate optimised model to isolate mathematical deficiencies.
3. Mathematically improve the predictive capabilities of the optimised model.
4. Compare prediction of improved model to optimised model and formulate conclusions on potential benefits.

5.2 Improved Ethyl model based on measured data

Regression techniques are used to develop correlations from data. In this project, non-linear regression techniques were used to optimise the Ethyl model's coefficients, based on the measured data. The measured data was obtained through CFR octane measurements and the predicted data were calculated using the Ethyl model. Please refer to Section 2.4.2 for a detailed explanation of the standard Ethyl model equations. Figure 5.1 presents a flowchart of the general approach used to optimised and improve the Ethyl model.

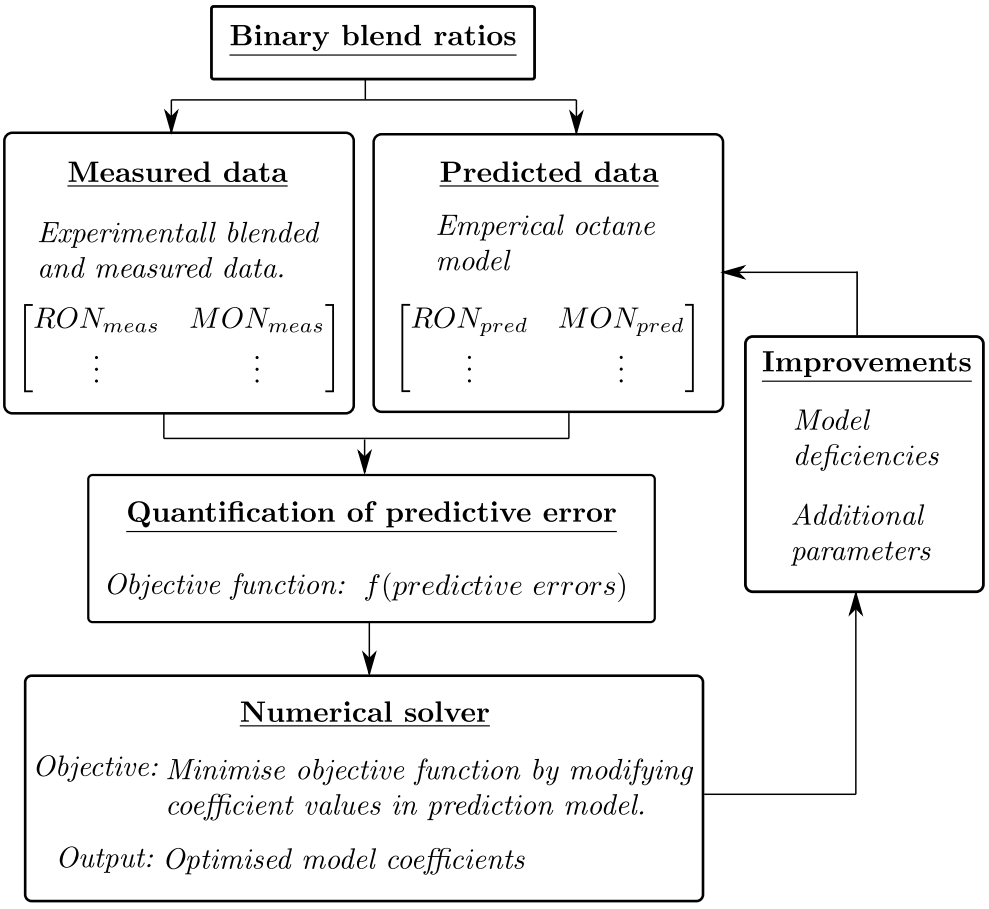

Figure 5.1: Optimisation flowchart.

MATLAB was used as the solver software, to minimise the objective function, by varying the predictive models coefficient values. The objective func-

tion describes the predictive error using the Euclidean vector norm, also called the L2 norm. The L2 norm was chosen because it targets larger errors in the data with more weighting. The initial coefficients used for the optimisation were the standard Ethyl coefficients (Healy *et al.*, 1959).

Possible outliers in the predicted data were identified by error magnitude, calculated using the L2 norm. All data points with an error value larger than the averaged predictive error value were re-measured (RON and MON) and accurately bracketed using PRFs. It was concluded that all possible outliers were indeed measured correctly, within the TSF specified tolerances.

The Ethyl model coefficients were optimised and the new optimised model showed improved predictive capabilities. The optimised coefficients are listed in Table 5.1.

Table 5.1: Coefficients for the standard, optimised and improved Ethyl models.

Coefficients	Ethyl	Optimised	Improved
a_1	0.03224	0.038608	0.34818
a_2	0.00101	0.00071881	0.00044721
a_3	0	-0.0025429	-0.0026397
a_4	N/A	N/A	0.001906
b_1	0.04450	0.055854	0.053704
b_2	0.00081	0.00085451	0.00069698
b_3	-0.00645	-0.016531	-0.017183
b_4	N/A	N/A	0.0054017

Table 5.2 listed the SEs for the standard and optimised Ethyl models.

Table 5.2: Standard errors (SE) of each prediction model.

SE	Standard Ethyl	Optimised Ethyl	Improved Ethyl
RON	5.49	3.09	1.39
MON	4.97	1.33	1.33

To further improve the predictive capabilities of this optimised model an additional term was added. The data was investigated to find that the largest predictive errors were mostly blends with alcohol content.

Therefore, a term describing alcohol content, with similar form to the olefin and aromatic terms in Equations 2.4 & 2.5, was added to the optimised model to give Equations 5.1 & 5.2. The alcoholic term is highlighted in Equations 5.1 & 5.2. These equations are referred to as the 'improved Ethyl model' in this report.

$$RON = \overline{r} + a_1(\overline{rj} - \overline{r}\overline{j}) + a_2(\overline{O^2} - \overline{O}^2) + a_3(\overline{A^2} - \overline{A}^2) + \boldsymbol{a_4(\overline{E^2} - \overline{E}^2)} \quad (5.1)$$

$$MON = \overline{m} + b_1(\overline{mj} - \overline{m}\overline{j}) + b_2(\overline{O^2} - \overline{O}^2) + b_3(\frac{\overline{A^2} - \overline{A}^2}{100})^2 + \boldsymbol{b_4(\frac{\overline{E^2} - \overline{E}^2}{100})^2} \quad (5.2)$$

Where, E is the alcohol content.

The new coefficients in Equations 5.1 & 5.2 were optimised using a similar approach as before. These coefficients are also listed in Table 5.1. Using Table 5.2, it is shown that the SEs for the improved model decreased significantly for the RON predictions, however, remained the same for the MON predictions.

Figure 5.2 shows the measured, original, optimised and improved Ethyl model RON predictions. Please note that only a portion of the data is presented in Figure 5.2, in order to show the various improvements more clearly.

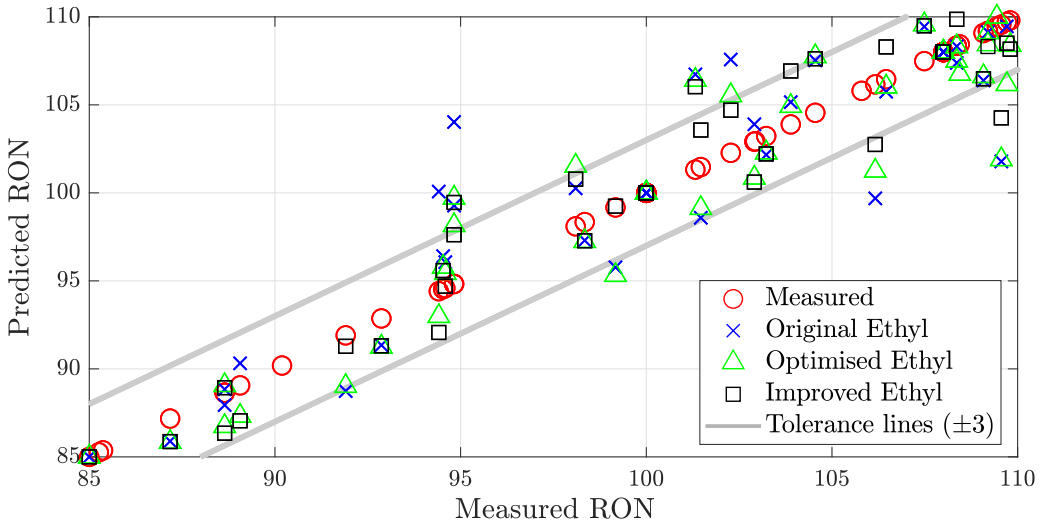

Figure 5.2: Comparison between standard, optimised and improved Ethyl RON models.

The horizontal axis is scaled according to the measured data, forcing the measured data to form a straight line. This is useful for comparing the predictions to the measured data as the vertical distance between the two is the predictive error. Two tolerance lines are also plotted in Figure 5.2 for magnitude reference purposes.

5.3 Summary

Table 5.2 and Figure 5.2 show that the improved Ethyl model better predicts the measured results for RON. As intended, the predictions with the largest error (vertical distance) were targeted and improved. For MON, no improvement is observed for the improved Ethyl model. It was concluded that the additional alcoholic term (added in Equation 5.2) did not influence the model's accuracy as much, because the L2 error magnitudes are much smaller in the MON case.

In summary, the measured data was used to successfully improve the predictive capabilities of the standard Ethyl model. Initially optimising the Ethyl model, allowed possible deficiencies to be identified and improved, to minimise the largest predictive errors. It is intended that this model has the potential to now fit larger refinery-specific data better after the model's coefficients have been robustly optimised to the data set and determined, since a possible deficiency has been identified and rectified.

Chapter 6

General Discussion

6.1 Overview

There is vast octane blending data for the selected components used for this project, some of which were reported in Chapters 2 & 3. However, much of this data stems from studies involving components blended into production fuels or its use as a petrol surrogate. These studies may provide useful insight into the component's pure octane data, but no useful insight for the binary combinations is gained. Added to this, only a small number of these studies experimentally measure RON and MON, using a CFR engine. Therefore, to the best of the author's knowledge, the literature cited throughout the report and in this chapter are valuable contributions to the field.

This chapter discusses the significance of the project results in the context of this report and important literature sources. It distinguishes between cases where the results met the project's expectations and situations with consistent or conflicting findings to literature as well as situations with no supporting literature.

The chapter begins by discussing the pure component results, after which the binary blend results are discussed. A discussion is formulated on the empirical Ethyl model's ability to match the experimental results as well as the improved octane predicting model developed in Chapter 5. It ends by discussing the potential value of having this better understanding of these new synergistic and antagonistic blending effects, obtained in this project.

6.2 Pure components

6.2.1 Consistent results to literature

As stated previously, the RON and MON values of the two PRFs, n-heptane and isooctane are defined by ASTM definition as zero and 100, respectively. Therefore, it is imperative to ensure their purities are according to ASTM specification. The isooctane used for testing was 99.47 % pure and the n-heptane 98.87 % pure.

The RON and MON of pure toluene were critical, as it formed part of the TSF fuels, used for qualifying the CFR engine during each operating period. Toluene was used to extend the measurable range of the CFR engine above a RON of 100, therefore, the RON of toluene was pre-defined using trusted literature. The American Petroleum Institute (1957), Obert (1973), Heywood (1988) and Foong *et al.* (2014) list a RON of 120 for pure toluene. The procured toluene for this project, was 99.01 % pure.

Significantly different MON values are reported for toluene. A report published by the ASTM Institute (1958) reports a MON of 103.5, Heywood (1988) and Obert (1973) report a MON of 109 and according to the measurements performed by Foong *et al.* (2014) and Bergenthuin (2018) a MON of 107 was obtained. A MON of 107 was measured in this project and was concluded satisfactory when compared to Foong *et al.* (2014) and Bergenthuin (2018).

While several RON and MON values have been reported for neat ethanol, it was concluded that the measurements obtained by Hunwartzen (1982), Anderson *et al.* (2012) and Foong *et al.* (2014) are the most reliable. This is due to their compliance with the ASTM standards and measurements were performed with the same ASTM prescribed CFR modifications discussed in Chapter 3. Also considering that the ASTM standards specify a TSF rating tolerance of $\pm$ 1.4 for RON and $\pm$ 0.4 for MON within this measurement range, a measured RON of 108 and MON of 90.2, was in good agreement with the literature mentioned here. Please refer to Table 4.1. The purity of the ethanol used in this study, was 99.91 % pure.

It was found that the RON and MON of high purity TAME was only reported by few literature sources, with a large range in values. Table 6.1 reports the RON and MON values for TAME.

Table 6.1: Reported RON and MON for neat TAME.

RON (±1.7)*	MON (±1.2)*	Reference
110.4	96.3	This study
105-115.6	95.7-104.5	Mirabella *et al.* (2016)
112	99	Botha *et al.* (2002)
112	98	Hamid and Ali (1995)

* TSF rating tolerance specified in brackets.

Mirabella *et al.* (2016) reports the few data collected for TAME and lists a range for possible RON values. This range is indicated in Table 6.1. Taking this range, the ASTM tolerances and literature values into account, it was concluded that the measured RON and MON values for TAME were satisfactory. The TAME used for testing was found to be 97.70 % pure.

6.2.2 Conflicting results to literature

In comparison with the values cited from literature, some of the neat component RON and MON results differed. Table 6.2 reports the RON and MON values for 1-hexene.

Table 6.2: Reported RON and MON for neat 1-hexene.

RON (±0.5)*	MON (±1.1)*	Reference
75.7	63.3	This study
76.4	63.4	API (1957)
76	63	Obert (1973)
73.6	64.5	Badra *et al.* (2017)
72.7		Yuan (2018)

* TSF rating tolerance specified in brackets.

The measured MON for 1-hexene matches the listed literature values very well. However, the RON differs from the cited values but does fall within the lowest and highest values found in literature. The 1-hexene was tested to be 96.61 % pure and was accurately bracketed using PRFs. The measured RON and MON values for 1-hexene were therefore considered satisfactory.

Table 6.3 reports the RON and MON values for cyclohexane.

Table 6.3: Reported RON and MON for neat cyclohexane.

RON (±0.3)*	MON (±0.3*)	Reference
83.7	79.9	This study
83	77.2	API (1957)
84	78	Obert (1973)
83	77.2	Guibet (1991)
82.2		Yuan (2018)

* TSF rating tolerance specified in brackets.

The measured RON for cyclohexane matches the listed literature values well, however, the MON value differs. Unfortunately, the recent study by Yuan (2018) did not measure the MON of cyclohexane. The cyclohexane was tested to be 98.80 % pure and was also accurately bracketed using the PRFs. The measured RON and MON values for cyclohexane were therefore considered satisfactory.

6.3 Binary blends

This study involved a large matrix of binary blend results. These results are graphed in Section 4.4.2. Table 6.4 categorises the binary blend results according to consistent or conflicting results to literature and unsupported cases. Of all the 21 binary combinations, 12 results are consistent with literature, three results show conflicts and six results are unsupported.

Table 6.4: Consistent, conflicting and unsupported cases with literature.

Component	hex	tol	eth	tame	iso	n-hep	cyc
1-hexene		✓	✓	♦	✘	♦	♦
toluene			✓	✓	✓	✓	✓
ethanol				✘	✓	✓	✓
TAME					♦	✘	♦
isooctane						✓	✓
n-heptane							♦
cyclohexane							

✓ Consistent
✘ Conflicting
♦ Unsupported

6.3.1 Consistent results to literature

The binary blending behaviours of the two PRFs, toluene and ethanol are popular choices to represent actual blending behaviours found in petrol. The two PRFs define the octane scale and represent the paraffin class well. Again, by definition, the PRFs blend perfectly linearly by volume. Therefore, these components are typical choices for the paraffinic ingredients. The same can be said for toluene and ethanol, both with well-established octane boosting and blending data.

Both Foong *et al.* (2014) and Yuan (2018) confirmed approximately linear blending for toluene in isooctane and n-heptane. Figure 4.7 confirms these linear octane responses, however, large antagonism is observed for the toluene/isooctane MON blending in Figure 4.7. Unfortunately, Yuan (2018) and Foong *et al.* (2014) did not measure the MON values for this blend, but Foong *et al.* (2014) does confirm antagonistic blending using a model proposed by Morgan *et al.* (2010).

Yuan (2018) measured the RON of toluene blended into 1-hexene and cyclohexane and concluded slight antagonistic blending for toluene/1-hexene and large antagonistic blending for toluene/cyclohexane. Figure 4.7 is consistent with these findings. Unfortunately, no literature was found to confirm the MON responses for these blends. Yuan (2018) also measured the RON of isooctane blended into cyclohexane. A linear blending response was observed for this blend and is consistent with this project's isooctane/cyclohexane measurements in Figure 4.10.

Foong *et al.* (2014) studied the octane blending effects of ethanol blended into n-heptane, isooctane and toluene and Yuan (2018) the blending effects of ethanol blended into 1-hexene and cyclohexane.

Figure 6.1 is repeated here, together with the measured results. Figure 6.1 confirms that the synergistic and antagonistic blending effects measured for ethanol and the mentioned components, are indeed consistent with those found in literature. A similar conclusion was drawn for the MON case for ethanol/n-heptane, ethanol/isooctane and ethanol/toluene blends (not plotted here).

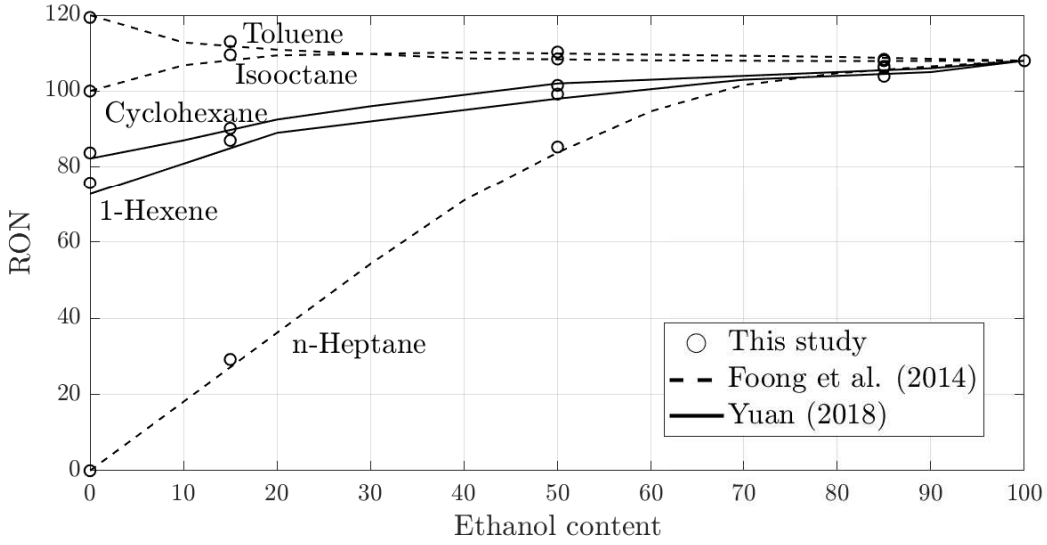

Figure 6.1: Measured RON for ethanol binary blends compared to those obtained by Foong *et al.* (2014) and Yuan (2018).

6.3.2 Conflicting results to literature

Botha *et al.* (2002) confirms synergistic blending between Sasol's SFA alcohol fuel blended with TAME. However, observation of Figure 4.9, shows that approximately linear blending behaviour was measured for the RON of ethanol blended into TAME. The MON case has a small antagonistic response over the entire composition. It can be argued that because SFA was used instead of neat ethanol, that the true blending behaviours of ethanol were not portrayed, even though the SFA fuel is 95 % neat ethanol and 5 % neat propanol. Nonetheless, this project has shown that small additions of components to a blend, can drastically alter the octane responses.

Conflicting RON blending results were obtained for ethanol/TAME, isooctane/1-hexene and n-heptane/TAME blends. Yuan (2018) found synergistic blending for the isocotane/1-hexene blend, however, this blend was found to show a combination of synergistic and antagonistic blending. Bergenthuin (2018) studied the suitability of using n-heptane to find the BON of TAME and

concluded a slight synergistic blending relationship for the RON of n-heptane blended into TAME. This study showed that a larger synergistic blending effect was found for this blend. For the MON case, Bergenthuin (2018) measured a slight synergism, which aligns with the measured results in Figure 4.9.

6.3.3 Unsupported binary blend results

To the best of the author's knowledge, no experimental RON and MON literature data was found for the unsupported blends listed in Table 6.4. This is of course extremely valuable to this research field, due to the fact that these binary measurements hold according to the ASTM standards and high purity neat components were used.

6.4 Ability of the empirical models to match experimental results

6.4.1 Standard Stewart and Ethyl models

Two well-established octane blending prediction models were investigated to determine their suitability in predicting the measured results. The predictions were graphed in Section 4.4.2 and it was shown, using SEs, that the Ethyl model was more capable in predicting the experimentally measured results. It was concluded that this was due to the fact that the Ethyl model includes additional parameters suitable for describing OS and aromatic non-linearities. The Stewart model only includes a non-linear parameter for olefin content, therefore the Stewart model becomes a LBV calculation when no olefin content is present in the blend.

It is challenging to draw definitive conclusions for octane number predictions of complex fuel mixtures, especially when uncommon and/or unstudied components are involved. However, it has been stated before, that the measured results are on a fundamental level. Therefore, this investigation into these predictive models provides insightful information in describing the non-linear blending among hydrocarbons and oxygenates, which are currently not accurately described.

6.4.2 Optimised and improved Ethyl model

The standard Ethyl model was optimised and then improved to better predict the measured RON and MON binary blend measurements. Initially, the standard Ethyl model coefficients were optimised and showed an improved SE over the standard Ethyl model. It was then decided to mathematically improve the model by using an additional term to describe the largest predictive errors

(largely blends with alcohol content) using this model. It was found that in the RON case the SE improved, however, no improvement was observed for the MON case. Table 6.5 is a repeat of Table 5.2, showing all the SEs of the various prediction models, but also including the SEs for the LBV calculations.

Table 6.5: Standard errors (SE) of listed prediction models.

SE	LBV	Stewart	Standard Ethyl	Optimised Ethyl	Improved Ethyl
RON	15.3	14.8	5.49	3.09	**1.39**
MON	9.4	11.7	4.79	**1.33**	**1.33**

The lowest SE for the RON predictions was that of the improved Ethyl model and for MON the optimised and improves models have the same SEs. These SEs are highlighted in bold text in Table 6.5. A SE of 1.4 RON and 1.3 for MON approaches the acceptable TSF rating tolerances specified in the ASTM standards.

One of the largest binary prediction errors was that of ethanol blended into isooctane. Figure 6.2 shows the predictions using the standard, optimised and improved Ethyl models for this blend.

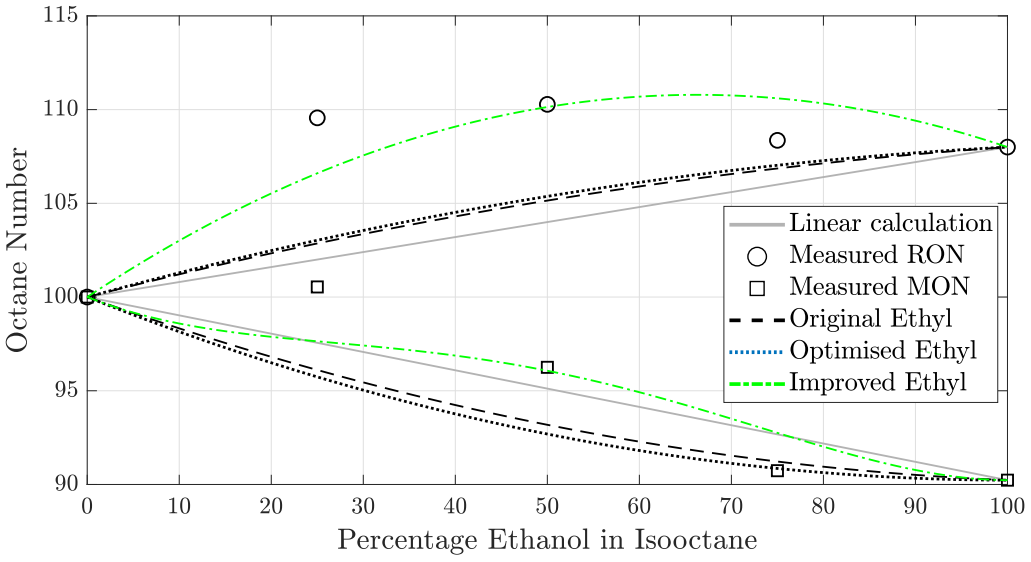

Figure 6.2: Predictions of ethanol/isooctane binary blends using standard, optimised and improved Ethyl models.

Figure 6.2 shows how the improved Ethyl model better predicts the measured RON and MON at the 50/50 midpoint point. This is an important finding because using the measured data and the additional alcoholic term, a much better prediction can be made for this binary blend. A similar result was obtained for the MON predictions.

6.5 Insights gained

Octane blending is known to exhibit non-linear synergistic and antagonistic interactions among the various constituent hydrocarbons and oxygenates of the petrol recipe (Scott, 1958). This makes it extremely difficult for fuel producers to accurately predict the octane of their FBR fuels, which leads to costly octane 'give-away' to safely meet local and international fuel specifications.

In order to assist Sasol in their octane predictive capabilities, the objectives of this project were defined to obtain and exploit non-linear synergistic and antagonistic octane blending behaviours of common component classes found in the petrol recipe. These efforts would then potentially assist in better octane enhancing and predicting powers.

Approximately every binary blend investigated in this project portrayed either synergistic and/or antagonistic octane blending. Use of these fundamental results, allows certain conclusions to be drawn pertaining to the required volume percentage of each component for a specific purpose. For example, in Figure 4.9, the RON of isooctane increases proportionally with the addition of TAME, but then decreases drastically with more than 50 % by volume of TAME. Added to this, the OS is largest at this 50/50 blend ratio. A discussion on the link between OS and modern SI fuels is discussed in Section 6.6.

The following insights can be formulated concerning the synergistic and antagonistic blending of the various component classes studied in this project:

1. It was found that most of the hydrocarbons blend synergistically with increasing alcohol content, except for the aromatic component toluene, which blended antagonistically. This shows that for various blends, the antagonism between ethanol and toluene will possibly act against the synergisms between ethanol and the other hydrocarbon classes in multi-component blends. A similar conclusion was drawn by Foong *et al.* (2014).

2. The general trend for olefinic blending was a synergistic response, except for toluene, which showed antagonistic blending for both RON and MON cases. Although the observed synergisms were small for each binary

blend, the general trend suggests that the olefin class either increases or maintains the LBV ON of the petrol recipe. In order to deduce more information on the blending ratios for maximum synergy, please refer to Figure 4.6.

3. As mentioned before, increasing aromatic content in alcohol and olefin fuels produces antagonistic octane blending. The same trend is observed for toluene/TAME and toluene/cyclohexane blends. However as expected, a linear response between toluene and the two PRFs is observed. Therefore, the general antagonisms relating to aromatic content requires careful attention.

4. TAME is used for octane enhancing properties, however, when blended into toluene or cyclohexane it blends antagonistically. This is important to know when dealing with high aromatic and cyclo-paraffin compositions. More importantly, for certain blend ratios, TAME exhibits a combination of synergistic and antagonistic blending. For example, additions of TAME up to 70 % in isooctane will blend synergistically, however after this ratio, it will blend antagonistically (Figure 4.9).

5. Another important finding between the synergism of TAME blended into isooctane, is that at the 50/50 blend ratio, the RON value of the binary blend approaches that of TAME. Therefore, one could obtain the RON value of TAME, in a paraffin-rich fuel, using this blend ratio. However, special attention must be placed on the volume addition of TAME, because the RON value decreases drastically after this 50/50 blend ratio. Please see Figure 4.9.

6. Careful attention must be placed on the blending of cyclohexane with aromatics and ethers, due to the antagonistic behaviours of these blends. Where not mentioned before, cyclohexane remained either linear or synergistic when blended with all of the other selected components.

6.6 Octane sensitivity (OS) and its link to spark ignition (SI) fuels

Section 2.2.3 highlighted that important insights can be formulated by studying the magnitude of the OS between each of the various binary blends. The OS is directly related to OI using a K value (Equation 2.1). Kalghatgi (2001*b*) confirms that modern SI engines prefer fuels with higher OSs and Yates *et al.* (2005) lists the suitability of fuels for non-carburettored engines, with turbo- or super-chargers, with respect to OS.

Therefore, by studying where the maximum RON and OS occurs in each of the measured binary blends, conclusions can be drawn on the blends suitability to modern downsized engines. Added to this, the binary results confirmed that in some cases, a combination of synergistic and antagonistic blending is present, showing that OS is dependent on blend ratio. This is extremely valuable because in some countries, limits are placed on the maximum allowable blend ratios for certain components, and knowing where the maximums occur is important. Please refer to Section 4.4.1 for a more detailed example explanation.

Using the measured binary blend RON and MON results and the above discussion, the following conclusions are drawn:

1. The OS remains constant for increasing olefin content in all the studied classes except for iso-paraffins and cyclo-paraffins. Observation of 1-hexene/isooctane and 1-hexene/cyclohexane blends in Figure 4.6, shows a large linear increase in OS with increasing olefin content. Therefore, high olefin content in these paraffinic fuels is more suitable to highly boosted modern engines. However, the low RON values counter this argument and the one made by Yates *et al.* (2005), in that high RON values are required. One could possibly use the synergism between 1-hexene and ethanol to increase this low RON value.

2. It is shown in Figure 4.7 that very large OS and high RON values are obtained for low toluene content up to 50 % when blended into ethanol, TAME and isooctane. These high OS and RON values align with the conclusions drawn by Kalghatgi (2001*b*) and Yates *et al.* (2005) and are thus highlighted here for their suitability in modern SI fuel recipes. The OS remains approximately constant for increasing toluene content blended into 1-hexene, TAME and in n-heptane. Added to this, the maximum allowable aromatic content in both Europe and the United States is 35% by volume, thus these conclusions are also relevant in regard to these limits (Kalghatgi and Stone, 2018).

3. Of particular interest in Figure 4.8 is the OSs between ethanol and TAME. Both RON and MON binary octane responses are linear, but the OS increases. Both ethanol and TAME are used extensively as octane enhancers, therefore, this linear blend relationship with increasing OS can be of use to refineries using both components in their specific fuel recipe. Large OSs were also observed between increasing alcohol content in isooctane and cyclohexane.

4. For TAME blended into isooctane, a synergistic response was observed for RON and an antagonistic response for MON. Together with this,

the OS was largest at the 50/50 blend ratio, where the synergistic RON value is almost equal to the RON value of neat TAME. This is an important finding because, the RON value of neat TAME can be achieved by blending it in a 50/50 ratio with isooctane and at this midpoint, the OS is maximised. This aligns well with the requirements of highly boosted, downsized SI engines.

5. The antagonistic blending behaviour for the MON of isooctane/TAME assists in the increase of the blend's OS at the 15/75 ratio. Both isooctane and toluene have been used extensively for petrol surrogate formation and in the ASTM reference fuel blends and knowing this information is valuable for future use and research into these important components

6. The OS of n-heptane binary blends were not as distinguishable as in other blends studied in this project. This could be due to the low temperature reactions that are defined by n-heptane predominantly and this reaction is scavenged when significant quantities of other components (e.g. ethanol) are present. Of interest is the constant RON value of the n-heptane/ethanol blend up to 15 % n-heptane addition. It is expected that the high RON value and the synergistic blending of ethanol forces the addition of the low octane paraffin to remain high until a sufficient volume percentage is added.

6.7 Other discussion points

6.7.1 Non-metallic octane booster (NMOB) characteristics

The NMOB 2,4-Xylidine was added to each of the selected components in one, two and three percentage by volume ratios, in order to isolate its octane boosting properties. Please refer to Section 4.6 for the graphed results. Measuring the RON and MON of neat 2,4-Xylidine is not within the measurable range of the CFR engine. The following conclusions can be drawn from the NMOB results:

1. The NMOB increases the RON of 1-hexene, isooctane, n-heptane and cyclohexane, whereas it decreased the RON of toluene. Addition of the NMOB to ethanol and TAME produced a linear response and there was no significant octane increase. This could be contributed to the fact that both ethanol and TAME are oxygenates, therefore it can be assumed that 2,4-Xylidine is not suitable for increasing the RON of oxygenates.

2. A large linear increase in RON values was observed for isooctane and the NMOB. This could be due to the stable nature of isooctane, with its

branched molecular structure. It was mentioned before that a branched molecular structure is more stable than a straight-chain molecule.

3. When the NMOB was added to n-heptane, a non-linear response was measured. Following the trend, in Point 2 above, it was concluded that this is attributed to the fact that n-heptane is a less stable component than isooctane.

4. The MON measurements showed less octane boosting characteristics, which is related to the more severe operating conditions. The NMOB increased the MON of 1-hexene, TAME, n-heptane and cyclohexane. The NMOB decreased the MON of toluene and isooctane and a linear response was observed for ethanol.

5. It is again observed that no significant octane increase is observed for the ethanol and TAME cases, further confirming the assumption made earlier.

6.7.2 RON and MON measurement drift

During the experimental testing phase, a measurement drift of up to 0.5 ONs was observed. Similar observations were made by Foong *et al.* (2014). It was concluded that the observed measurement drift was due to increased combustion chamber deposits during the commencement of the testing program (Stott, 1978). It is emphasised that while measurement drift was present, the CFR engine was qualified for each operating period by performing the fit-for-use TSF tests. These tests confirmed that the observed measurement drift remained within the ASTM rating tolerances.

6.8 Discussion of project hypothesis

Both the hypothesis and foundational assumption were presented in Chapter 1. In the context of the project's foundational assumption, this project's hypothesis is supported by the project results and the discussions provided in this chapter. It was shown that non-linearities do exist between binary combinations of common fuel classes found in the SI fuel recipe and that more than one non-linearity (synergism and antagonism) can exist in such a blend.

Although only binary blending interactions were investigated in this project, one could hypothesise that similar non-linear blending behaviours may exist between other examples of the same chemical class, or hypothesise that the modelled fits to these binary behaviours could be used in trinary and more complex blends. Nonetheless, the foundational data obtained from this project provides a platform for steering current and future research to ultimately provide refinery prediction and operational value.

Chapter 7

Conclusions

This chapter concludes the report and provides important conclusions that were obtained throughout the completion of this project.

The following conclusions were drawn on the non-linear octane blending behaviours found between each of the binary blends:

1. A synergistic and antagonistic octane blending behaviour can both exist in a fuel blend.
2. The antagonism between ethanol and toluene suggests that, for specific volumetric blend ratios, toluene can act against the synergisms found between ethanol and other hydrocarbon classes in a multi-component blend. The antagonism between toluene and TAME shows that using TAME to boost the octane of an aromatic-rich fuel, will possibly decrease the octane of such a blend.
3. The significant non-linearities found for ethanol in 1-hexene, toluene, isooctane and cyclohexane are more significant at low ethanol concentrations by volume, concluding that even at low concentrations, ethanol significantly influences the octane number of a blend.
4. Blending ethanol and TAME by volume indicates that these oxygenates, interact linearly with respect to octane behaviour, similar to that observed for hydrocarbon components of the same class.
5. Binary blends containing 1-hexene, show a linear or slight synergistic blending response, suggesting that the olefin class either maintains or increases both the RON and MON of the blend.
6. The synergistic blending response found for low TAME concentrations are typically followed by an antagonistic blending response for the higher

TAME concentrations. However this was not the case for TAME in ethanol and in n-heptane.

The following conclusions were drawn concerning the link between octane sensitivity (OS) and modern spark ignition (SI) engines:

1. It was concluded that OS is a function of blend ratio and it is desired, for modern SI engines, to use fuel components that demonstrate a synergistic behaviour for RON and antagonistic behaviour for MON to maximise the OS.
2. At various blend ratios, isooctane was found to synergistically increase the RON and antagonistically decrease the MON value when blended into toluene, ethanol and also in TAME. Similar results were found for ethanol in TAME and in cyclohexane.
3. Binary blends with high concentrations of 1-hexene or n-heptane, showed consistently low OS values. Therefore, these blends containing a high olefin or paraffin content may require additional components to increase the OS.

The following conclusions were drawn on the octane boosting capabilities of the NMOB 2,4-Xylidine:

1. Influences the RON value more than the MON value of a blend.
2. The RON and MON of 1-hexene, n-heptane and cyclohexane, were increased, whereas the RON and MON of toluene decreased.
3. It increases the RON but decreases the MON of isooctane.
4. It had no influence on the RON and MON of ethanol and TAME.

The following conclusions were drawn on the ability of the empirical models to predict octane:

1. The standard Ethyl model was unable to predict accurately the RON and MON of blends with a high alcohol content.
2. Using optimisation techniques, an improved Ethyl model was able to better predict the RON and MON of all the blends tested in this project.

Chapter 8

Recommendations

This research has met the project's objectives and a number of satisfactory preliminary results but has also highlighted several areas for possible future research.

The following recommendations are made for future research in line with this project:

1. Modification steps have been taken to allow in-cylinder pressure measurements to be acquired during octane experiments. It is recommended to correlate in-cylinder pressures to the analogue knock intensity detonation meter readings, in order to draw similarities between the ASTM prescribed equipment and in-cylinder pressures.

2. It is recommended to test alternative choices for chemical class components, to provide certainty on which components do represent their respective hydrocarbon and oxygenate classes well and those which do not.

3. This project investigated non-linearities between binary combinations of common fuel components found in the SI fuel recipe. It is therefore recommended to investigate trinary combination blends based on the most important non-linear behaviours concluded in this project.

4. It is recommended to measure the torque during octane measurements using the dynomometer's torque arm and a load cell. Torque measurements, together with in-cylinder pressures, may provide valuable data for energy density calculations and insights into a fuel's energy density and its link to octane.

5. It is recommended to investigate possible trends in fuel component classes, octane and the recorded air-fuel ratio data for each of the binary blends measured in this project.

The following recommendations are made for future improvements to Stellenbosch University's CFR octane rating engine setup:

1. A measurement drift was observed throughout the completion of the testing matrix. It is recommended to clean the combustion chamber of any deposits before the commencement of any future projects.
2. It is recommended to implement a tachometer generator to provide closed-loop feedback for automatic dynomometer speed control to maintain constant RON and MON operating speeds.
3. Commissioning of a third fuel reservoir is also recommended, to improve the time efficiency of the bracketing methods, which require three fuel reservoirs.

Appendices

Appendix A

Experimental setup used for octane testing

The following chapter details all important hardware and software used for the experimental setup of Stellenbosch University's CFR octane rating engine.

A.1 CFR experimental setup

Research octane number (RON) and motor octane number (MON) tests were performed using Stellenbosch University's Cooperative Fuels Research (CFR) F1/F2 octane rating engine. Although this CFR engine was uniquely modified, all modifications and standardisation checks were performed according to the ASTM D2699 (for RON) and D2700 (for MON) standards and included adherence to the compression pressure requirements.

Table A.1 lists all of the important characteristics of Stellenbosch University's CFR engine setup, which are not listed in the ASTM standards (ASTM (2019*a*,*b*)) or in the ASTM manual for rating motor fuels by motor and research methods ASTM (1959).

Table A.1: Important characteristics of Stellenbosch University's CFR engine setup.

Item	Description
Engine	CFR F1/F2 Octane rating engine (Detonation engine #228773)
DAC[a]	National Instruments DAC, #NI USB-6216
PLC[b]	Allen-Bradley, Micro 830
Detonation pickup	Waukesha engine division, Model D1, #14221
Detonation meter	Weston instruments division, Model 271
Lambda scanner	ETAS Lambda-Anzeige scanner
Lambda sensor	Bosch lambda probe, #LSM 11, 12 V
Dynomometer	Wadkin & Co. DC motor #B28879
Temperature controllers	RKC REX-S100
IAT heater	1080 Watt, 230 V Coil heater
MIXT internal heater	4 ABSO 275 Watt, 230 V (9x200 mm)
MIXT band heater	800W, 230 V Band heater manufactured by Swift Heat & Control
AVL shaft encoder	0.2 °intervals

[a] Data acquisition unit.
[b] Programmable logic controller.

A.1.1 Electronic ignition system (EIS)

The spark timing is automatically adjusted (dependent on the CR) on modern CFR engines. Unfortunately, these adjustments must be made manually using Stellenbosch University's CFR engine. Therefore, as per the recommendations by Bergenthuin (2018), an electronic ignition system (EIS) using an engine control unit (ECU) was implemented. This eliminated the extra time required for timing adjustments and proved valuable to the project's timeline. Table A.2 lists the components which make up the EIS.

Table A.2: Components which make up the electronic ignition system.

Item	Description
ECU	Perfect Power Model XMS5B-8A
Charge amplifier	Perfect Power Blue Fire, 4 Channel
Trigger wheel	60-2 machined trigger wheel

The trigger wheel supplies the ECU with the piston position, via a crankshaft position sensor. The trigger wheel allows for accurate angle ad-

justment in order to postilion the wheel at the TDC position. An additional sensor was implemented to measure the crank position, eliminating wasted spark. The Perfect Power ECU unit uses LetRipp Technology software, allowing the user to set up and tune various engine parameters.

A.2 Thermocouple calibration

Various temperatures were carefully controlled during octane measurements in accordance with the ASTM standards, and to insure that healthy operation of the engine is maintained. The intake air temperature (IAT), mixture temperature (MIXT), coolant, oil, exhaust and ambient temperatures were measured by J-type and K-type thermocouples and the PLC listed in Table A.1. A LabView program converts the PLC data into presentable data for the operator via a graphical user interface (GUI). The GUI also provides information for speed readings.

The thermocouples were calibrated using a Fluke 9142 Fiel Metrology Well (#B29291). Provision was made in the GUI to easily calibrate the temperature readings. This calibration process was performed by Bergenthuin (2018) and in the present study.

A.3 Gravimetric blending setup

Liquid fuel test samples were blended using a gravimetric blending approach as outlined in the ASTM standards (ASTM, 2019*a*,*b*). Two digital scales, blending software and the appropriate glassware were used to blend test samples within a 0.2 % by mass, tolerance limit (ASTM, 2019*a*,*b*). Both scales can measure to an accuracy of 0.01 g.

The blending software used for the blending of liquid samples was developed by Dr. Gareth Floweday. Microsoft Excel, together with Visual Basic, was used to read real-time mass measurements from the digital scale. A GUI allows the user to easily understand the operation of the software and to accurately blend fuels with up to three components, in the order that they are added to the blend. The blending software takes ambient temperature, fuel densities and expansion coefficients into account.

Special care must be taken when obtaining the fuel densities, as the density of a fuel is dependent on temperature and fuel composition. Density values may be obtained from the fuel manufacturers or reputable literature sources. Each of the densities was calculated using Perry's Chemical Engineers' Handbook (Perry and Green, 1963) and then compared to the manufacturer listed values.

Appendix B

Generation of a characteristic curve (CC)

It was required to generate a characteristic curve (CC) for both research octane number (RON) and motor octane number (MON) for Stellenbosch University's CFR engine. A CC forms part of the compression ratio (CR) procedure prescribed by the ASTM D2699 and D2700 standards. In order to qualify the CCs, the fit-for-use toluene standardised fuel (TSF) tests were measured using the CFR engine and the results were interpolated using the CCs. Generating a CC that produces accurate TSF results, for the entire TSF range was a large iterative exercise. This chapter discusses the various engine specific test features, which played an important role in maintaining the ASTM specified operating conditions.

B.1 Spark energy

As per the ASTM standards, ignition must be electronically triggered through an ignition coil to the spark plug. The spark plug must be a Champion D16, or equivalent (ASTM, 2019*a*,*b*). It was found that the observed knock intensity (KI) during an octane measurement was affected by the spark energy, i.e., by the supplied coil voltage. Added to this: the ignition coil would become sufficiently hot during long operating periods. This was attributed to the high duty cycle of the original mechanical points ignition system on the CFR engine. This duty cycle was essentially inverted when a new electronic ignition system (EIS) was implemented on the CFR engine and therefore, the coil remained at room temperature during long operating periods.

Regardless of whether the mechanical or electronic system is used, the supplied coil voltage remains the same. The ASTM standards specify that the coil voltage must remain at 12 V (ASTM, 2019*a*,*b*). It was observed that small

variances in coil voltages altered the KI readings. In order to investigate the dependence of KI on the coil voltage, standard KI was obtained for isooctane and the coil voltage was adjusted in small increments. TableB.1 lists the KI for small changes in coil voltage.

Table B.1: KI readings for changing ignition coil voltages, whilst measuring isooctane.

Coil voltage (V)	KI (Divisions)
11	42
11.5	45
12	50
13	52

Table B.1 concludes that special care must be taken to ensure that the supplied coil voltage remains at 12 V.

The influence of the dwell time on KI readings was also investigated, using the EIS. It was found that the dwell time did not influence the KI readings with dwell times between 3 ms to 15 ms. A value of 6 ms was selected for the dwell time.

B.2 Speed control

The current speed control system requires the operator to continuously monitor and alter the operating speed of the dynamometer using the supplied voltage to the dynamometers drive system. This could potentially lead to an incorrect octane measurement and wasted test fuel samples.

The dynamometer drive system uses the armature voltage as the feedback condition for speed control. However, when the armature temperature increases during operation, so does its resistance and therefore the current decreases. The drive system counters this set point change by increasing the operating speed, which in turn requires the users input to change the voltage supplied to the drive system. This makes it challenging for the user over long operating periods, because continuous monitoring and voltage adjustments are required. In order to improve this system, an external tachometer generator could be used to supply closed loop feedback control, which is independent of the armature voltage.

B.3 Spark timing

It was found that undesirable electrical noise caused incorrect spark timing, when using the new EIS system. It is believed that the high switching voltage and current on the feed to the dynomometer and the observed sparking on the commutator (when the motor was absorbing the combustion from CFR engine) was the source of this interference. It was concluded that this noise caused incorrect measurements of the toothed wheel, resulting to incorrect firing patterns. In order to counteract any electrical noise, the correct shielded wiring was implemented, after which, no variation in spark timing was observed.

Appendix C

Experimental data

The following chapter includes the raw data obtained from experimental measurements using Stellenbosch University's CFR octane rating engine. It begins by listing the toluene standardised fuels (TSF) test results as well as the results used for the RON and MON characteristic curves (CC) generation. It then lists the RON and MON results for the pure component and binary testing phases. It then ends by presents the raw measured RON and MON of a non-metallic octane booster (NMOB).

C.1 Characteristic curve (CC) and toluene standardised fuel (TSF) tests

The engine specific CFR RON or MON CC is generated by measuring the RON and MON of various blended primary reference fuels (PRFs) and plotting these results against the corresponding corresponding compression ratios (CR). The dial gauge readings on Stellenbosch University's CFR engine was calibrated to the corresponding CR via the liquid fill method (Bergenthuin, 2018). Table C.1 lists the data points used to generate the RON and MON CCs.

Table C.1: Characteristic curve data.

RON	Dial[a]	CR	MON	Dial	CR
10.00	1.1	5.12	10.00	1.03	5.12
20.00	1.05	5.2	20.00	0.99	5.2
30.00	0.99	5.2	30.00	0.95	5.25
40.00	0.93	5.23	40.00	0.90	5.28
50.00	0.88	5.25	50.00	0.86	5.32
60.00	0.82	5.42	55.00	0.83	5.39
70.00	0.76	5.65	60.00	0.81	5.43
80.00	0.71	5.89	63.00	0.79	5.52
83.00	0.68	6.04	70.00	0.74	5.71
90.00	0.62	6.43	80.00	0.65	6.26
92.00	0.60	6.57	82.00	0.61	6.47
94.00	0.57	6.79	85.00	0.56	6.83
95.00	0.55	6.92	90.00	0.50	7.37
96.00	0.53	7.05	92.50	0.45	7.86
98.00	0.50	7.38	95.00	0.44	7.96
100.00	0.45	7.77	100.00	0.39	8.46
108.00	0.35	9.09	107.00	0.34	9.16
120.00	0.25	10.89			

[a] Dial gauge reading in inches.

According to the ASTM standards. each operating period shall use a qualified CFR engine, by performing TSF tests that must fall within certain tolerances ASTM (2019*a*,*b*). Table C.2 lists the TSF test results used to qualify the CC for RON and MON measurements. In addition to this, each operating period was qualified by blending and testing TSF fuels relevant to the octane range to be tested. These results are not included here.

Table C.2: Toluene standardised fuels (TSF) results to qualify CC curves.

TSF	Tolerance[a]	RON*	TSF	Tolerance[a]	MON*
65.1	± 0.6	65.0	58	± 1.1	58.3
75.6	± 0.5	75.9	66.9	± 1.1	67.6
85.2	± 0.3	85.7	74.8	± 1	75.1
89.3	± 0.3	89.6	78.2	± 0.3	77.8
93.4	± 0.3	93.2	81.5	± 0.3	81.2
96.9	± 0.3	96.5	85.2	± 0.3	85.5
99.8	± 0.3	99.5	88.7	± 0.3	88.2
103.3	± 0.9	102.9	92.6	± 0.4	92.0
107.6	± 1.4	109.0	96.6	± 1.2	97.3
113	± 1.7	113.0	99.8	± 0.9	99.5
			100.8	± 1.3	101.3

[a] Tolerances specified in ASTM standards (ASTM, 2019*a*,*b*).
* Meaured RON and MON.

C.2 Pure component results

Table C.3 lists the measured RON and MON values for the components selected for this project. Both RON and MON values of n-heptane and isooctane are equal (zero octane sensitivity) and are defined by ASTM definition as 100 and zero, respectively. The measurable range of Stellenbosch University's CFR engine did not allow the testing of pure n-heptane.

Table C.3: Measured and reported RON and MON of neat components.

Component	Measured RON	AFR*	Measured MON	AFR
1-Hexene	75.7	0.94	63.3	0.95
Toluene	120	0.99	107	1.05
Ethanol	108	0.93	90.2	0.95
TAME	110.4	0.96	96.3	1.03
Isooctane	100	0.92	100	1.03
n-Heptane	0		0	
Cyclohexane	83.7	1.02	79.9	1.00

*Air-fuel ratio.

C.3 Binary blend results

The following Tables list the RON and MON measurements of all the binary blends tested in this project. Please refer to each table heading for RON/MON

and component reference. Please note the following:

1. The table caption refers to the component that is blended to the components in each table row. For example, Table C.4 lists all of the 1-hexene RON binary blends, where each row is a specific component that 1-hexene is blended into at the specified ratios.
2. The ratios are in volume percentages and are defined by A/B, where A is the component blended into component B. For example using the first row in Table C.4, a ratio of 25/75 is 25 % 1-hexene and 75 % toluene.
3. The extremes of the compositions (0/100 and 100/0) are the pure RON or MON values measured for each of the components.
4. The blend ratios were altered after the 1-hexene binary blends to better represent refinery blend ratios.
5. The AFR is provided in square brackets.

C.3.1 RON binary results

Table C.4: 1-Hexene binary blend RON measurement results.

Blend ratio	0/100	25/75	50/50	75/15	100/0
Toluene	119.4	102.9 [1.00]	94.4 [0.97]	84.9 [0.94]	75.7
Ethanol	108.0	103.9 [0.98]	99.2 [1.00]	90.2 [0.98]	75.7
TAME	110.4	101.3 [0.98]	94.6 [0.95]	85.4 [0.94]	75.7
Isooctane	100.0	94.5 [0.94]	88.6 [0.92]	82.2 [0.92]	75.7
n-Heptane	0.0	23.0 [0.92]	41.8 [0.92]	64.3 [0.94]	75.7
Cyclohexane	83.7	82.4 [1.01]	79.6 [1.00]	77.1 [0.94]	75.7

Table C.5: Toluene binary blend RON measurement results.

Blend ratio	0/100	15/85	50/50	85/15	100/0
1-Hexene	75.7	84.9 [0.94]	94.4 [0.97]	102.9 [1.00]	119.4
Ethanol	108.0	109.7 [0.98]	108.4 [0.95]	113.0 [0.99]	119.4
TAME	110.4	109.2 [1.00]	109.8 [0.99]	114.1 [1.00]	119.4
Isooctane	100.0	102.9 [0.91]	110.3 [0.94]	115.4 [1.00]	119.4
n-Heptane	0.0	17.9 [0.92]	65.2 [0.94]	102.3 [1.00]	119.4
Cyclohexane	83.7	89.1 [1.02]	94.8 [1.00]	105.8 [1.00]	119.4

Table C.6: Ethanol binary blend RON measurement results.

Blend ratio	0/100	15/85	50/50	85/15	100/0
1-Hexene	75.7	90.2 [0.98]	99.2 [1.00]	103.9 [0.98]	108.0
Toluene	119.4	113.0 [0.99]	108.4 [0.95]	109.7 [0.98]	108.0
TAME	110.4	109.4 [0.98]	109.2 [0.97]	108.4 [0.90]	108.0
Isooctane	100.0	109.6 [1.01]	110.3 [0.96]	108.4 [0.95]	108.0
n-Heptane	0.0	25.0 [0.92]	85.3 [0.96]	106.2 [0.93]	108.0
Cyclohexane	83.7	91.9 [1.01]	101.5 [0.99]	106.5 [0.97]	108.0

Table C.7: TAME binary blend RON measurement results.

Blend ratio	0/100	15/85	50/50	85/15	100/0
1-Hexene	75.7	85.4 [0.94]	94.6 [0.95]	101.3 [0.98]	110.4
Toluene	119.4	114.1 [1.00]	109.8 [0.99]	111.8 [1.00]	110.4
Ethanol	108.0	108.4 [0.90]	109.2 [0.97]	109.4 [0.98]	110.4
Isooctane	100.0	103.2 [0.94]	109.1 [0.95]	107.5 [0.96]	110.4
n-Heptane	0.0	14.7 [0.92]	65.2 [0.93]	98.1 [0.94]	110.4
Cyclohexane	83.7	88.6 [1.00]	94.8 [1.00]	104.6 [1.00]	110.4

Table C.8: Isooctane binary blend RON measurement results.

Blend ratio	0/100	15/85	50/50	85/15	100/0
1-Hexene	75.7	82.2 [0.92]	88.6 [0.92]	94.5 [0.94]	100.0
Toluene	119.4	115.4 [1.00]	110.3 [0.94]	102.9 [0.91]	100.0
Ethanol	108.0	108.4 [0.95]	110.3 [0.96]	109.6 [1.01]	100.0
TAME	110.4	107.5 [0.96]	109.1 [0.95]	103.2 [0.94]	100.0
n-Heptane	0.0	15.0 [0.92]	50.0 [0.92]	85.0 [0.92]	100.0
Cyclohexane	83.7	87.2 [1.02]	92.9 [0.99]	98.3 [0.98]	100.0

Table C.9: n-Heptane binary blend RON measurement results.

Blend ratio	0/100	15/85	50/50	85/15	100/0
1-Hexene	75.7	64.3 [1.00]	41.8 [0.92]	23.0 [0.94]	0.0
Toluene	119.4	102.3 [1.00]	65.2 [0.94]	17.9 [0.92]	0.0
Ethanol	108.0	106.2 [0.93]	85.3 [0.96]	25.0 [0.92]	0.0
TAME	110.4	98.1 [0.94]	65.2 [0.93]	14.7 [0.92]	0.0
Isooctane	100.0	85.0 [0.92]	50.0 [0.92]	15.0 [0.92]	0.0
Cyclohexane	83.7	74.7 [0.99]	52.8 [0.95]	13.1 [0.92]	0.0

Table C.10: Cyclohexane binary blend RON measurement results.

Blend ratio	0/100	15/85	50/50	85/15	100/0
1-Hexene	75.7	77.1 [0.94]	79.6 [1.00]	82.4 [1.01]	83.7
Toluene	119.4	105.8 [1.00]	94.8 [1.00]	89.1 [1.02]	83.7
Ethanol	108.0	106.5 [0.97]	101.5 [0.99]	91.9 [1.01]	83.7
TAME	110.4	104.6 [1.00]	94.8 [1.00]	88.6 [1.00]	83.7
Isooctane	100.0	98.3 [0.98]	92.9 [0.99]	87.2 [1.02]	83.7
n-Heptane	0.0	13.1 [0.92]	52.8 [0.95]	74.7 [0.99]	83.7

C.3.2 MON binary results

Table C.11: 1-Hexene binary blend MON measurement results.

Blend ratio	0/100	15/85	50/50	85/15	100/0
Toluene	107.0	96.8 [1.05]	79.9 [1.00]	66.8 [0.95]	63.3
Ethanol	90.2	92.1 [0.96]	82.6 [0.98]	70.3 [1.00]	63.3
TAME	96.3	92.2 [1.00]	82.7 [1.03]	70.3 [1.05]	63.3
Isooctane	100.0	88.8 [1.02]	80.7 [0.96]	67.4 [1.02]	63.3
n-Heptane	0.0	17.6 [0.92]	37.2 [0.95]	55.0 [0.92]	63.3
Cyclohexane	79.9	78.5 [1.00]	72.6 [1.00]	65.1 [1.00]	63.3

Table C.12: Toluene binary blend MON measurement results.

Blend ratio	0/100	15/85	50/50	85/15	100/0
1-Hexene	63.3	66.8 [0.95]	79.9 [1.00]	96.8 [96.75]	107.0
Ethanol	90.2	91.3 [1.00]	92.3 [0.95]	99.2 [1.00]	107.0
TAME	96.3	99.3 [0.97]	93.2 [1.00]	100.0 [1.02]	107.0
Isooctane	100.0	102.2 [1.02]	100.0 [1.03]	102.2 [1.00]	107.0
n-Heptane	0.0	20.0 [0.92]	56.3 [0.90]	98.3 [1.00]	107.0
Cyclohexane	79.9	80.3 [1.02]	82.8 [1.02]	90.5 [1.03]	107.0

Table C.13: Ethanol binary blend MON measurement results.

Blend ratio	0/100	15/85	50/50	85/15	100/0
1-Hexene	63.3	70.3 [1.00]	82.6 [0.98]	92.1 [0.96]	90.2
Toluene	107.0	99.2 [1.00]	92.3 [0.95]	91.3 [1.00]	90.2
TAME	96.3	94.3 [0.98]	92.3 [1.01]	90.3 [0.94]	90.2
Isooctane	100.0	100.5 [1.02]	96.3 [1.02]	90.7 [1.02]	90.2
n-Heptane	0.0	29.6 [0.94]	80.1 [0.95]	87.7 [0.96]	90.2
Cyclohexane	79.9	82.0 [0.96]	85.3 [1.00]	87.1 [0.95]	90.2

Table C.14: TAME binary blend MON measurement results.

Blend ratio	0/100	15/85	50/50	85/15	100/0
1-Hexene	63.3	70.3 [1.05]	82.7 [1.03]	92.2 [1.00]	96.3
Toluene	107.0	100.0 [1.02]	93.2 [1.00]	99.3 [0.97]	96.3
Ethanol	90.2	90.3 [0.94]	92.3 [1.01]	94.3 [0.98]	96.3
Isooctane	100.0	99.7 [1.00]	95.0 [1.00]	96.8 [1.00]	96.3
n-Heptane	0.0	24.6 [0.91]	64.5 [0.92]	90.9 [0.99]	96.3
Cyclohexane	79.9	81.4 [0.96]	85.8 [0.96]	90.9 [0.97]	96.3

Table C.15: Isooctane binary blend MON measurement results.

Blend ratio	0/100	15/85	50/50	85/15	100/0
1-Hexene	63.3	67.4 [1.02]	80.7 [0.96]	94.5 [1.02]	100.0
Toluene	107.0	102.2 [1.00]	100.0 [1.03]	102.2 [1.02]	100.0
Ethanol	90.2	90.7 [1.02]	93.5 [1.02]	100.5 [1.02]	100.0
TAME	96.3	96.8 [1.00]	95.0 [1.00]	99.7 [1.00]	100.0
n-Heptane	0.0	15.0 [0.92]	50.0 [0.90]	85.0 [0.92]	100.0
Cyclohexane	79.9	80.8 [1.00]	86.1 [0.97]	92.3 [0.99]	100.0

Table C.16: n-Heptane binary blend MON measurement results.

Blend ratio	0/100	15/85	50/50	85/15	100/0
1-Hexene	63.3	55.0 [0.92]	37.2 [0.95]	17.6 [0.92]	0.0
Toluene	107.0	98.3 [1.00]	56.3 [0.90]	20.0 [0.92]	0.0
Ethanol	90.2	87.7 [0.96]	80.1 [0.95]	29.6 [0.94]	0.0
TAME	96.3	90.9 [0.99]	64.5 [0.92]	24.6 [0.91]	0.0
Isooctane	100.0	85.0 [0.92]	50.0 [0.90]	15.0 [0.92]	0.0
Cyclohexane	79.9	73.9 [0.99]	44.8 [0.90]	19.3 [0.92]	0.0

Table C.17: Cyclohexane binary blend MON measurement results.

Blend ratio	0/100	15/85	50/50	85/15	100/0
1-Hexene	63.3	65.1 [1.00]	72.6 [1.00]	78.5 [1.00]	79.9
Toluene	107.0	90.5 [1.03]	82.8 [1.02]	80.3 [1.02]	79.9
Ethanol	90.2	87.1 [0.95]	85.3 [1.00]	82.0 [0.96]	79.9
TAME	96.3	90.9 [0.97]	85.8 [0.96]	81.4 [0.96]	79.9
Isooctane	100.0	92.3 [0.99]	86.1 [0.97]	80.8 [1.00]	79.9
n-Heptane	0.0	19.3 [0.92]	44.8 [0.90]	73.9 [0.99]	79.9

C.4 Non-metallic octane booster (NMOB) results

The octane boosting capabilities of a non-metallic octane booster, 2,4-Xylidine was investigated. The NMOB was added to the selected components in 1, 2 and 3 percentage by volume ratios.

Table C.18 and Table C.19 list the measured RON and MON results.

Table C.18: NMOB RON results.

% NMOB	1	2	3
1-Hexene	76.9 [0.9]	83.7 [1]	87.5 [0.9]
Toluene	114.7 [1.02]	114.5 [0.9]	114.2 [1.02]
Ethanol	107.9 [0.99]	108.4 [0.97]	108.1 [0.97]
TAME	109.4 [0.98]	110.4 [0.99]	110.6 [0.99]
Isooctane	104.3 [0.92]	108.8 [0.92]	112.9 [0.97]
n-Heptane	12 [0.93]	31.5 [0.93]	40.3 [0.92]
Cyclohexane	88.3 [1]	89.3 [1.04]	92.5 [1.04]

Table C.19: NMOB MON results.

% NMOB	1	2	3
1-Hexene	67 [1]	70.4 [1]	73.9 [1]
Toluene	105.4 [1.02]	102.4 [1.03]	102.4 [1.03]
Ethanol	89.8 [1]	90.2 [0.94]	90.2 [0.92]
TAME	97 [0.96]	97 [0.96]	97.3 [0.96]
Isooctane	99.5 [1.02]	98.8 [1.03]	99.1 [1.03]
n-Heptane	17.8 [1]	23.4 [1.01]	34.3 [1.01]
Cyclohexane	79.9 [1.01]	80.6 [1.02]	80.8 [1.02]

Table C.20: RON measurements for NMOB blended into commercial ULP.

% NMOB	0	1	2	3	5
Source 1	95	97.38	98.78	100.3	102.4
Source 2	95	97.4	98.69	100.2	102.6

Table C.21: MON measurements for NMOB blended into commercial ULP.

% NMOB	0	1	2	3	5
Source 1	85	86.6	88.6	90.2	93
Source 2	85	86.2	88.7	90.3	92.5

List of References

AlRamadan, A.S., Sarathy, S.M., Khurshid, M. and Badra, J. (2016). A blending rule for octane numbers of prfs and tprfs with ethanol. *Fuel*, vol. 180, pp. 175–186.

American Petroleum Institute (1957). *A.P.I. Research Project 45, American Petroleum Institute Hydrocarbon Research Project, the Ohio State University Research Foundation*. No. v. 1 in A.P.I. Research Project 45.
Available at: `https://books.google.co.za/books?id=AWHkNwAACAAJ`

Anderson, J., Kramer, U., Mueller, S. and Wallington, T. (2010). Octane numbers of ethanol- and methanol- gasoline blends estimated from molar concentrations. *Energy & Fuels*, vol. 24, no. 12, pp. 6576–6585.

Anderson, J.E., Leone, T.G., Shelby, M.H., Wallington, T.J., Bizub, J.J., Foster, M., Lynskey, M.G. and Polovina, D. (2012). Octane numbers of ethanol-gasoline blends: measurements and novel estimation method from molar composition. Tech. Rep., SAE Technical Paper.

ASTM (1959 April). Astm manual for rating motor fuels by motor and research methods. American Society for Testing and Materials, Philadelphia, U.S.A.

ASTM (2019*a*). *D2699-19, Standard Test Method for Research Octane Number of Spark-Ignition Engine Fuel, ASTM International, West Conshohocken, PA, 2019, www.astm.org*.

ASTM (2019*b*). *D2700-19, Standard Test Method for Motor Octane Number of Spark-Ignition Engine Fuel, ASTM International, West Conshohocken, PA, 2019, www.astm.org*.

Badra, J., AlRamadan, A.S. and Sarathy, S.M. (2017). Optimization of the octane response of gasoline/ethanol blends. *Applied Energy*, vol. 203, pp. 778–793.

Bergenthuin, J.G. (2018). *High octane and oxygenated test setup for CFR octane engine*. Master's thesis, Department of Mechanical and Mechatronic Engineering, University of Stellenbosch.

Blackmore, D.R. (1977). *Fuel economy of the gasoline engine: fuel, lubricant and other effects*. Springer.

Boot, M.D., Tian, M., Hensen, E.J. and Sarathy, S.M. (2017). Impact of fuel molecular structure on auto-ignition behavior–design rules for future high performance gasolines. *Progress in Energy and Combustion Science*, vol. 60, pp. 1–25.

Botha, J.J., Strauss, H., Roets, P., Van Heerden, J., Healy, W., Maassen, C. and Peterson, R. (2002 November). Accurate determination of ether/alcohol octane synergies in specified base fuel matrices. *XIV International Symposium on Alcohol Fuels ISAF*, pp. 12–15.

Cengel, Y.A. (2015). *Thermodynamics: an engineering approach*. Eighth edition. edn. ISBN 9789814595292.

da Silva Jr, A., Hauber, J., Cancino, L. and Huber, K. (2019). The research octane numbers of ethanol-containing gasoline surrogates. *Fuel*, vol. 243, pp. 306–313.

Daly, S.R., Niemeyer, K.E., Cannella, W.J. and Hagen, C.L. (2016). Predicting fuel research octane number using fourier-transform infrared absorption spectra of neat hydrocarbons. *Fuel*, vol. 183, pp. 359–365.

Edgar, G. (1927). Measurement of knock characteristics of gasoline in terms of a standard fuel. *Industrial & Engineering Chemistry*, vol. 19, no. 1, pp. 145–146.

Foong, T.M., Morganti, K.J., Brear, M.J., da Silva, G., Yang, Y. and Dryer, F.L. (2014). The octane numbers of ethanol blended with gasoline and its surrogates. *Fuel*, vol. 115, pp. 727 – 739. ISSN 0016 - 2361.

Gheorghiu, V. (2012). Ultra-downsizing of internal combustion engines. In: *Sustainable Automotive Technologies 2012*, pp. 145 – 155. Springer.

Guibet, J. (1991 December). *Fuels and Engines*. Revised ed. edn. Editions Technip, Paris, France. ISBN ISBN: 10 2710807548.

Hamid, S.H. and Ali, M.A. (1995). Effect of mtbe blending on the properties of gasoline. *Fuel science & technology international*, vol. 13, no. 5, pp. 509–544.

Healy, W., Maassen, C. and Peterson, R. (1959). A new approach to blending octanes. In: *Proc. 24th Meeting API Refining Division*, vol. 39, pp. 132–136.

Heywood, J.B. (1988). *Internal combustion engine fundamentals*. McGraw-Hill's AccessEngineering, second edition. edn.

Hoth, A., Gonzalez, J.P., Kolodziej, C.P. and Rockstroh, T. (2019). Effects of lambda on knocking characteristics and ron rating. Tech. Rep., SAE Technical Paper.

Hunwartzen, I. (1982). Modification of cfr test engine unit to determine octane numbers of pure alcohols and gasoline-alcohol blends. Tech. Rep., SAE technical paper.

IEA, I.E.A. (2019). *CO2 emissions from fuel combustion 2019 edition*. IEA CO2 emissions from fuel combustion database.
Available at: `http://wds.iea.org`

Institute, A.P. (1958). Knocking characteristics of pure hydrocarbons. American Society for Testing Materials.

Johnson, R.T. and Riley, R.K. (1976). Single cylinder spark ignition engine study of the octane, emissions, and fuel economy characteristics of methanol-gasoline blends. Tech. Rep., SAE Technical Paper.

Kalghatgi, G. (2001*a*). Fuel anti-knock quality-part i. engine studies. *SAE Transactions*, pp. 1993–2004.

Kalghatgi, G., Head, R., Chang, J., Viollet, Y., Babiker, H. and Amer, A. (2014). An alternative method based on toluene/n-heptane surrogate fuels for rating the anti-knock quality of practical gasolines. *SAE International Journal of Fuels and Lubricants*, vol. 7, no. 3, pp. 663–672.

Kalghatgi, G. and Stone, R. (2018). Fuel requirements of spark ignition engines. *Proceedings of the Institution of Mechanical Engineers, Part D: Journal of Automobile Engineering*, vol. 232, no. 1, pp. 22 – 35.

Kalghatgi, G.T. (2001*b*). Fuel anti-knock quality-part ii. vehicle studies-how relevant is motor octane number (mon) in modern engines? *SAE Transactions*, pp. 2005–2015.

Kalghatgi, G.T. (2014). *Fuel/engine interactions*. ISBN 9780768064582.

Kenny, W.J. (2013). *Development of an engine testing facility for spark ignition engine fuels*. Ph.D. thesis, Mecahnical and Mechatronic Engineering, Stellenbosch University.

Konig, G. and Sheppard, C. (1990). End gas autoignition and knock in a spark ignition engine. *SAE transactions*, pp. 820–839.

Leppard, W.R. (1990). The chemical origin of fuel octane sensitivity. *SAE transactions*, pp. 862–876.

Midgley Jr, T. and Boyd, T. (1922). Methods of measuring detonation in engines. *SAE Transactions*, pp. 126–140.

Miller, J.A. and Fisk, G.A. (1987). Combustion chemistry. *Chem. Eng. News*, vol. 65, no. 35, pp. 22 – 46.

Millo, F., Ferraro, C., Barbera, E. and Margaria, G. (1995). Octane rating methods at high revolution speed. Tech. Rep., SAE Technical Paper.

Mirabella, W., Avella, F., Di Girolamo, M., Abbott, T. and Busch, O. (2016). Blending octane evaluation of fuel ethers: A literature review. Tech. Rep., SAE Technical Paper.

Mittal, V. and Heywood, J.B. (2008). The relevance of fuel RON and MON to knock onset in modern SI engines. Tech. Rep., SAE Technical Paper.

Mittal, V. and Heywood, J.B. (2010). The shift in relevance of fuel RON and MON to knock onset in modern SI engines over the last 70 years. *SAE International Journal of Engines*, vol. 2, no. 2, pp. 1–10.

Morgan, N., Smallbone, A., Bhave, A., Kraft, M., Cracknell, R. and Kalghatgi, G. (2010). Mapping surrogate gasoline compositions into ron/mon space. *Combustion and Flame*, vol. 157, no. 6, pp. 1122–1131.

Morris, W.E. (1975). The interaction approach to gasoline blending. In: *NPRA Paper AM-75-30, National Petroleum Refiners Association annual meeting.*

Obert, E.F.E.F. (1973). *Internal combustion engines and air pollution.* Intext series in mechanical engineering. HarperCollins, New York, N.Y. ISBN 0700221832.

Perez, P.L. and Boehman, A.L. (2012). Experimental investigation of the autoignition behavior of surrogate gasoline fuels in a constant-volume combustion bomb apparatus and its relevance to hcci combustion. *Energy & fuels*, vol. 26, no. 10, pp. 6106–6117.

Perry, R.H. and Green, D.W. (1963). *Chemical engineers' handbook.* McGraw-Hill series in chemical engineering. McGraw-Hill handbooks. International student edition, 4th edn. McGraw-Hill, New York, N.Y.

Richards, P. (2014). *Automotive fuels reference book.* Third edition. edn. ISBN 9780768006384.

Rockstroh, T., Kolodziej, C.P., Jespersen, M.C., Goldsborough, S.S. and Wallner, T. (2018). Insights into engine knock: Comparison of knock metrics across ranges of intake temperature and pressure in the cfr engine. *SAE International Journal of Fuels and Lubricants*, vol. 11, no. 2018-01-0210, pp. 545–561.

Ronney, D.P. (2013). *AME 436 - Lecture 10 - Combustion engines presentation.*

Scott, E. (1958). Knock characteristics of hydrocarbon mixtures. *Proc. API DiV. Refin*, vol. 38, p. 90.

Stewart, W.E. (1959). Predict octanes for gasoline blends. *Petroleum Refiner*, vol. 38, no. 12, pp. 135–139.

Stott, G. (1978). *A guide to operational and maintenance problems on ASTM-CFR engines*, vol. 80. Alberta Research Council.

Stratiev, D., Nikolaychuk, E., Shishkova, I., Bonchev, I., Marinov, I., Dinkov, R., Yordanov, D., Tankov, I. and Mitkova, M. (2017). Evaluation of accuracy of literature gasoline blending models to predict octane numbers of gasoline blends. *Petroleum Science and Technology*, vol. 35, no. 11, pp. 1146–1153.

Swarts, A. (2006). *Insights relating to octane rating and the underlying role of autoigntion.* Ph.D. thesis, Department of Mechanical Engineering, University of Cape Town.

Swarts, A., Yates, A., Viljoen, Carl and Coetzer, R. (2005). A further study of inconsistencies between autoignition and knock intensity in the cfr octane rating engine. *SAE transactions*, pp. 702–720.

Swarts, A., Yates, A., Viljoen, C. and Coetzer, R. (2004). Standard knock intensity revisited: Atypical burn rate characteristics identified in the cfr octane rating engine. Tech. Rep., SAE Technical Paper.

Twu, C. and Coon, J. (1998). A generalized interaction method for the prediction of octane numbers for gasoline blends. *Simulation Science Inc*, pp. 1–18.

Viljoen, C. (2009). *Assessment of disparate strategies for octane prediciton*. Ph.D. thesis, Department of Chemical Engineering, University of Cape Town.

Yates, A.D., Swarts, A. and Viljoen, C.L. (2005). Correlating auto-ignition delays and knock-limited spark-advance data for different types of fuel. *SAE transactions*, pp. 735–747.

Yuan, H. (2018). *Octane blending and oxidation chemistry of ethanol-hydrocarbon mixtures*. Ph.D. thesis, Department of Mechanical Engineering, University of Melbourne.